ACS Catalysis

pubs.acs.org/acscatalysis Perspective

Perspective on Sorption Enhanced Bifunctional Catalysts to Produce Hydrocarbons

Seongbin Jo, Luz Cruz, Soham Shah, Somchate Wasantwisut, Annette Phan, and Kandis Leslie Gilliard-AbdulAziz*

Cite This: *ACS Catal.* 2022, 12, 7486−7510

Read Online

ABSTRACT: Sorption-enhanced catalysts are bifunctional materials consisting of a heterogeneous catalyst affixed to a solid sorbent with a combined capacity to selectively capture and convert CO_2 directly to value-added fuels and chemicals in the same reactor. The benefits of facile separation of CO_2, directly from air or from flue gas, and conversion to chemical commodities is appealing for developing an integrated carbon capture and utilization scheme. The growth of this area is rapidly expanding with interest from catalysis, materials design, and life-cycle analysis researchers. However, the promise of sorption-enhanced catalysts is limited by their reduced thermal stability, CO_2 capture capacity, and restricted product streams to C_1 hydrocarbons. The prime issue is that the reaction conditions for the capture of CO_2, regeneration of the sorbent, and utilization can be vastly different. It remains a challenge to optimize both the properties of the sorbent support material and the heterogeneous catalyst used. This perspective summarizes the current state-of-the-art for the properties of solid sorbents, heterogeneous catalysts, and the combined sorbent-enhanced catalysts for producing hydrocarbons from CO_2. Lastly, the perspective discusses challenges and future areas for improving the performance and capture efficiency of sorption-enhanced catalysts.

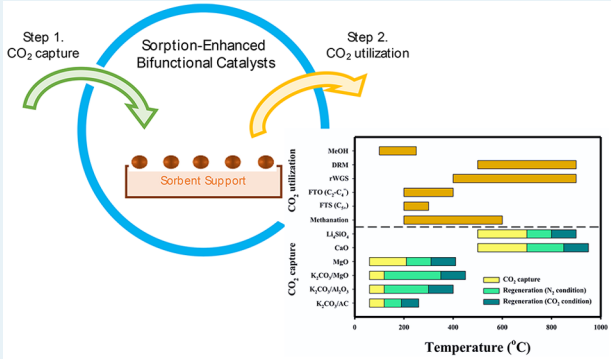

KEYWORDS: *integrated carbon capture and utilization, sorption-enhanced catalysts, carbon capture and utilization, carbon−carbon coupling, hydrocarbons*

1. INTRODUCTION

The technological development of our society from the start of the industrial revolution to now has resulted in increased emissions of greenhouse gases (GHGs), such as CH_4[1−3] and CO_2, in the atmosphere.[4,5] For instance, the emissions of CO_2 have, on average, increased by about 20 ppm per decade since 2000 and have now surpassed a total concentration in the atmosphere of 419 ppm.[6] With the increase of CO_2 and CH_4, the planet's surface temperature has increased rapidly, approaching an increase of the global surface temperature to 1.2 °C, the highest since the preindustrial era.[6] Additionally, a higher concentration of CO_2 in the atmosphere is associated with acidifying natural sinks such as oceans[7,8] and causing other adverse impacts to ecological and environmental domains.[9−11] To reduce GHG emissions, there have been efforts to develop negative emission technologies that take advantage of CO_2 capture and storage, or CCS, where CO_2 is captured and permanently stored using mineralization.[12] Combining CCS with CO_2 capture and utilization (CCU) provides a sustainable approach to closing the carbon cycle where CO_2 is converted and temporarily stored as chemical commodities and fuels.

The chemical industry is one of the most significant contributors to GHG emissions due to conventional processes that rely on oil and fossil resources.[13] A sustainable solution to maintain the chemical industry while reducing GHG emissions is using CO_2 as a potential feedstock for polymers,[14−18] chemicals,[19−24] and fuels.[13,25,26] Such a transition will use catalysts to provide a technologically practical solution for mitigating GHGs. While there are several thermo- and electro-catalytic CCU schemes,[16,27−33] the integration of heterogeneous catalysts with CO_2-capture solid sorbents may be a viable solution capable of selectively removing CO_2 directly from air or flue gases. The advantages of processes that utilize integrated CO_2 capture and utilization (ICCU) or sorption-enhanced catalysts (SECs) are the theoretical lower costs and process simplification, where separation of CO_2 can occur directly from

Received: April 5, 2022
Revised: May 24, 2022
Published: June 9, 2022

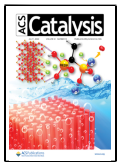

https://doi.org/10.1021/acscatal.2c01646
ACS Catal. 2022, 12, 7486−7510

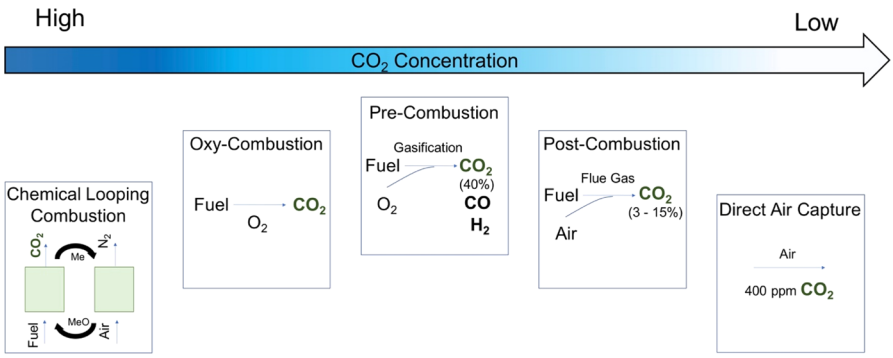

Figure 1. Schematic of carbon capture pathways for the capture and utilization of carbon dioxide from different streams.

gas streams and can be converted to value-added products.[34−36] Thus, technologies that rely on SECs eliminate the need for CO_2 storage sites and the formation of a pipeline network. This perspective examines the challenges of using sorption-enhanced catalysts and their potential to use captured CO_2 to produce hydrocarbons as an alternative carbon source. This perspective is useful to spur research in heterogeneous catalysis areas that can progress CCU and ICCU on the technology readiness scale.

There has been limited implementation of SEC strategies with commercial success due to the limited performance of the catalysts and solid sorbents used. The structure of CO_2 is stable and kinetically inert, and thus electrocatalytic, or thermocatalytic transformation usually requires high energy input. Solid sorbents with basic characteristics have high efficiency and selectivity to bind and capture CO_2 due to the inherent weak acidity of the CO_2.[37−39] The solid sorbents used, such as metal oxides,[37,40−46] zeolites,[38,47,48] and silicates[49−51] must have extraordinary stability to withstand impurities (H_2O, H_2S), humidity, and constant temperature fluxes. Typically, the medium to high temperatures and repeated cycling between carbonation (CO_2 adsorption) and calcination (CO_2 desorption) accelerate the sintering of the solid sorbent reducing the performance of the material over time. Coupling heterogeneous catalysts with solid sorbents presents unique challenges that must be tackled to drive research efforts toward the efficient and commercialized conversion of CO_2 to value-added chemicals. Thus, it is essential to develop active, selective, and stable heterogeneous catalysts coupled with robust solid sorbents while gaining insights into CO_2 transformation in various catalytic environments.

Typical thermal CO_2 conversion schemes use renewable hydrogen from water electrolysis as a reductant to synthesize relevant building blocks like synthesis gas (CO, H_2), methane, and methanol.[19,20,24,27,32,52−54] Most research using an ICCU framework has traditionally focused on C_1 products. However, the development of ICCU that can capture and convert CO_2 to C_2^+ hydrocarbons could be transformative. CO_2 conversion to C_2^+ hydrocarbons provides an environmentally friendly way for deriving essential building blocks of the chemical industry. However, one of the significant challenges for thermal conversion schemes is the high barrier for C−C coupling to synthesize C_2^+ molecules. Hydrocarbons, such as ethylene, are key feedstocks in the chemical industry to manufacture various chemicals and polymers. Ethylene is currently produced worldwide as a feedstock for various chemicals, plastics, paints, textiles, and packaging. Naphtha cracking is the primary source of industrial ethylene supply.[55,56] The naphtha-based cracking process is capital and energy-intensive and is a sizable GHG emitter. Improving the efficiency of SECs to C_2^+ hydrocarbons could be economically competitive and provide substantial reductions in greenhouse gas emissions.

This perspective communicates a broad understanding of how catalysts and solid sorbents are developed for SECs, where the subsequent utilization step goes beyond C_1 products. We describe knowledge gleaned from relevant publications on solid sorbents and heterogeneous catalysts with a primary focus on thermal conversion. The perspective sections describe aspects of solid sorbent design and the development of catalysts to synthesize hydrocarbon products. The perspective introduces these topics separately as initially sorbent development, catalyst development, and finally, the combination of the catalysts and sorbent to produce hydrocarbons. We address the role of the sorbent properties and the catalysts and the synergistic nature of the relationship so that the catalyst-sorbent behavior can advance. Finally, we summarize our discussions and outline emerging opportunities and pressing needs to develop SECs to open the door to more valuable chemical intermediates.

2. SORBENT-BASED CO_2 CAPTURE TECHNOLOGIES

CO_2 capture using solid sorbents involves either physisorption, surface adsorption by weak van der Waal forces, or chemisorption, where CO_2 binds to the surface through chemical bonds. Some solid sorbents used to capture and convert CO_2 usually operate at elevated temperatures (above 100 °C) and generally have a reduced regeneration energy penalty compared to other capture technologies. There are several pathways in which solid sorbents have been used to capture CO_2, including precombustion (CO_2 capture from reforming or syngas),[57,58] postcombustion (CO_2 capture from flue gas),[38,59] and oxyfuel-combustion (CO_2 capture from combusted fuel).[60] Additional capture strategies from CO_2 emission sources include chemical looping combustion (CLC) and direct air capture (DAC) (Figure 1).[61] The sorbent properties are contingent on the operating conditions (concentration of CO_2, temperatures, pressures) and are highly dependent on CO_2 capture pathways and fuel combustion sources.[61]

Precombustion CO_2 capture is based on the scaled industrial production of hydrogen and chemicals (e.g., fuel-cell or integrated gasification combined cycle (IGCC) plants).[62,63] In the precombustion process, the fuel sources (pulverized coal or natural gas) are converted with limited oxygen or water vapor into syngas using either partial oxidation, steam reforming, or autothermal reforming. The formed CO and H_2O are converted downstream to CO_2 and H_2 using the water−gas shift reaction (WGS). Before the H_2-rich fuel is combusted or the syngas is

https://doi.org/10.1021/acscatal.2c01646
ACS Catal. 2022, 12, 7486−7510

Table 1. Comparison of Material Properties of Select Solid Metal Oxide and Carbonate Sorbents for CO_2 Capture

materials	reaction mechanism	molecular weight (g/mol)	theoretical CO_2 capture capacity (mmol CO_2/g sorbent)	equilibrium temperature (°C) PCO_2 = 0.1/1.0 bar	melting point temperature (°C)
Na_2CO_3	$Na_2CO_3 + CO_2 + H_2O \leftrightarrow 2NaHCO_3$	106.0	9.44	90/110	Na_2CO_3: 851 $NaHCO_3$: decompose before melting
K_2CO_3	$K_2CO_3 + CO_2 + H_2O \leftrightarrow 2KHCO_3$	138.2	7.24	120/150	K_2CO_3: 900 $KHCO_3$: decompose before melting
MgO	$MgO + CO_2 \leftrightarrow MgCO_3$	40.30	24.8	255/310	MgO: 2852 $MgCO_3$: 990
Li_4SiO_4	$Li_4SiO_4 + CO_2 \leftrightarrow Li_2CO_3 + Li_2SiO_3$	119.8	8.34	575/725	Li_4SiO_4: 1258
CaO	$CaO + CO_2 \leftrightarrow CaCO_3$	56.08	17.8	755/895	CaO: 2572 $CaCO_3$: 1339
SrO	$SrO + CO_2 \leftrightarrow SrCO_3$	103.6	9.65	1050/1220	SrO: 2530 $SrCO_3$: 1495
BaO	$BaO + CO_2 \leftrightarrow BaCO_3$	153.3	6.52	>1200	BaO: 1973 $BaCO_3$: 1555

utilized, the concentrated CO_2 (15−50 vol % CO_2 at a pressure range from 0.5 to 10 bar) is removed. The removal of CO_2 helps achieve a high yield of H_2 production or to adjust the H_2-to-CO ratio.[63] The capture or removal of CO_2 during precombustion is considered more efficient to postcombustion technologies, but the investment and operating costs of the gasification process are often more expensive than those of traditional pulverized coal power plants.[62]

The postcombustion CO_2 capture method can be applied to conventional coal- or gas-fired power plants. According to the type of fuel used, CO_2 concentrations in the flue gas can range from 3 to 15 vol %. For example, the composition of the gas-fired flue gas was between 7.4 and 7.7% CO_2, 14.6% H_2O, ∼4.45% O_2, and 73−74% N_2.[64,65] While the composition of the coal-fired flue gas was 12.5−12.8% CO_2, 6.2% H_2O, ∼4.4% O_2, and 76−77% N_2.[64,65] A number of industries, including the cement, iron, or steel plants, have excessive CO_2 emissions from mineral conversion, and CO_2 concentrations can reach up to 35−40% in flue gas composition.[66] Ideally, CO_2 should be removed entirely from the flue gas before being released into the atmosphere to minimize GHG emissions. However, the major challenges for postcombustion CO_2 capture are the large amounts of CO_2 in the flue gas at essentially atmospheric pressures and in the temperature range of ∼100−150 °C. The presence of SOx, NOx, water vapor, and O_2 in the flue gas are additional problems for implementation, leading to a technical challenge for developing a cost-effective CO_2 capture process and properties of the sorbent.

Oxy-combustion involves the combustion of fuel feedstocks with pure oxygen, resulting in a pure stream of CO_2 after drying, cleaning, compression, and distillation of the flue gas.[67] In an air separation unit, substantial amounts of oxygen are separated from the air using either cryogenic distillation, polymeric membranes, or temperature swing adsorption (TSA) and pressure swing adsorption (PSA). One of the operational challenges is the high cost and energy consumption of oxygen from the air and the development of advanced combustors to mitigate high heat loads. After CO_2 formation, the CO_2 is purified and compressed for storage.

The CLC has been studied extensively for power generation using a dual fluidized bed system, an oxidizer, and a reducer, for an integrated CO_2 capture process. In the CLC process, oxygen carriers, usually metal oxides, undergo cyclic redox reactions between two reactors.[68] In the oxidizer reactor, the oxygen carriers first provide their lattice oxygen under low oxygen partial pressure conditions to combust hydrocarbon fuels providing condensed CO_2, while oxygen carriers are reduced to metal or less oxidized state. The reduced oxygen carriers are subsequently exposed to an oxidant such as air or water to supply oxygen in the lattice.

For the solid sorbent approach, CO_2 interacts with the solid material and is removed from the air mixture. Current research efforts are studying structures such as metal−organic frameworks (MOFs), zeolites, and activated carbon as viable solid sorbents that enhance physisorption or chemisorption. DAC is gaining attention as a complementary approach to processes that capture CO_2 from more concentrated sources like flue gas. In the DAC process, CO_2 is removed from the atmosphere containing approximately 400 ppm of CO_2 concentration.[69] DAC has the advantage of location flexibility and an input gas stream with low impurities such as SOx and NOx. Nevertheless, a diluted CO_2 concentration in the air is a disadvantage for efficient CO_2 capture technology, resulting in more energy-intensive than concentrated CO_2 sources.[61]

2.1. CO_2 Capture Solid Sorbents. In this perspective, we address the solid metal oxide sorbents for CO_2 capture by chemical adsorption that have been combined with heterogeneous catalysts for SECs. Albeit, there are other solid sorbents, including physical adsorption using activated carbon and carbon nanomaterials,[70] graphite/graphene,[71] zeolites adsorbents,[72] MOFs,[73] and chemical adsorption using amine-supported silica adsorbents.[74−76] The materials discussed below can be used for DAC, pre-, and postcombustion CO_2 capture. In practice, however, several sorbents would be thermodynamically favored at one specific application based on the temperature ranges, pressures, CO_2 concentration in the feed gas, and impurities such as water vapor, O_2, SOx, and NOx (Table 1).

For solid metal oxide sorbents, the maximum temperatures of carbonation and decarbonation are determined by the corresponding equilibrium CO_2 partial pressure of solid sorbents. The thermodynamic equilibrium was calculated by the Gibbs free energy minimization method using the HSC chemistry software. In Figure 2, we show that the PCO_2 and temperature above the equilibrium CO_2 partial pressure lines can influence the thermodynamic favorability of the oxide sorbents for CO_2 capture. The solid sorbents are thermodynami-

https://doi.org/10.1021/acscatal.2c01646
ACS Catal. 2022, 12, 7486−7510

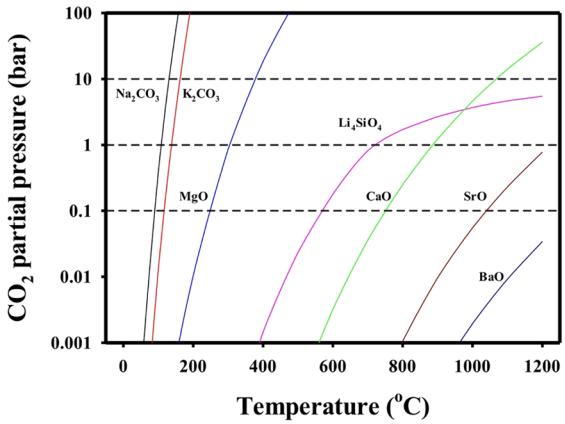

Figure 2. Graph of the thermodynamically favorable use of solid sorbents as a function of the partial CO_2 pressure (PCO_2) vs temperature (K_2CO_3, Na_2CO_3, MgO, Li_2SiO_3, CaO, SrO, BaO).

cally favorable for carbonation above the PCO_2 partial pressure line. While below the curve, the decarbonated phase is stable. The adsorption of CO_2 is mainly attributed to the weakly acidic nature of the molecule, where adsorption to alkali metal oxides, alkaline earth metal oxides, and alkali metal carbonate is facile and efficient.

Generally, the solid sorbents for CO_2 capture have been classified according to their sorption and desorption temperatures: (1) alkali metal carbonates are preferred for low temperatures below 200 °C, (2) MgO and hydrotalcites are preferred for intermediate temperatures between 200 and 400 °C, and (3) Li ceramics and CaO-based sorbents are preferred for high temperatures above 400 °C.[77] Typically, ICCU strategies use SECs with high-temperature sorbents due to their enhanced stability at temperatures to convert CO_2 to chemical commodities. Some alkali metal oxides (Na_2O and K_2O) and alkaline metal oxides (SrO and BaO) are not typically used as solid sorbents because of their extremely high carbonation and decarbonation temperatures (>900 °C). In addition to thermodynamic equilibriums, the solid sorbents should be selected by evaluating several factors such as the theoretical and experimental CO_2 capture capacity, CO_2 selectivity, sorption/desorption kinetics, mechanical strength, chemical stability, tolerance to impurities, regeneration energy, and sorbent cost.[78]

2.1.1. Low Temperature. Low-temperature CO_2 solid sorbents, such as alkali metal carbonate-based sorbents (M_2CO_3, M = K, or Na), have been widely investigated with high CO_2 capture capacity and low cost at temperatures below 200 °C.[79] These sorbents can be applied for CO_2 capture from the flue gas of fossil fuel-fired power plants at low temperatures between 100 and 150 °C.[64] In the chemical adsorption of CO_2, the alkali metal carbonate reacts with CO_2 and water vapor at 40−80 °C to form an alkali metal bicarbonate ($M_2CO_3 + CO_2 + H_2O \leftrightarrow 2MHCO_3$). In comparison, decarbonation occurs at around 120 °C.[80] Recently, the low-temperature CO_2 capture sorbents have been widely studied for the DAC process.[81,82] Despite the advantage of low-temperature carbonation and decarbonation, the common problem is that the overall carbonation reaction using alkali metal carbonates is relatively slow. Researchers have tried to improve Na_2CO_3-based sorbents using different precursors (Na_2CO_3, $NaHCO_3$), but the CO_2 capture kinetics and capacity are still unsatisfactory at low temperatures compared to the K_2CO_3-based sorbents.[83] To improve the heat transfer and to fluidize the solid particles for maximum CO_2 capture, the CO_2 capture and regeneration properties of K_2CO_3 have been widely investigated in a circulated fluidized bed process.[84,85] The studies showed that the fluidizer decreased the regeneration energy and improved the sorbent stability in dry and hydrous conditions (Figure 3).

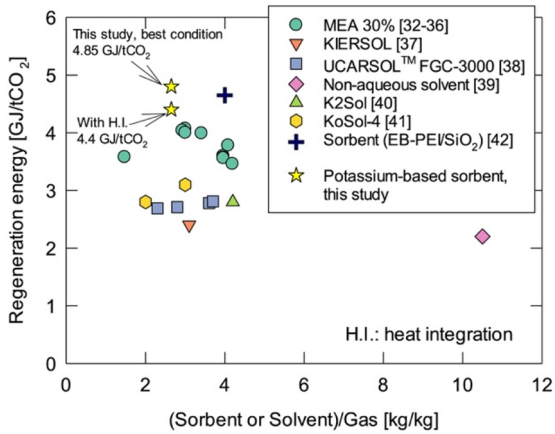

Figure 3. Comparison of the regeneration energy for K_2CO_3 in a bubbling fluidized reactor compared to other CO_2 capture technologies. Reproduced with permission from Reference 84. Copyright 2020, Elsevier.

Many researchers have attempted to resolve the slow kinetics by dispersing the active alkali metal carbonate on porous materials such as activated carbon,[81,86] TiO_2,[79,87] MgO,[88,89] and Al_2O_3,[85,90−92] leading to an enhanced sorption rate and mechanical strength required for usage in a fluidized bed or transport reactor. Lee et al. reviewed the CO_2 capture capacity and regeneration properties of K_2CO_3-based sorbents using different support materials (activated carbon, TiO_2, ZrO_2, Al_2O_3, MgO, and CaO).[79] However, several sorbents formed solid byproducts during the carbonation, such as $KAl(CO_3)_2(OH)_2$ in K_2CO_3/Al_2O_3 sorbent, $K_2Mg(CO_3)_2$, and $K_2Mg(CO_3)_2{\cdot}4(H_2O)$ in K_2CO_3/MgO sorbent, and $K_2Ca(CO_3)_2$ in K_2CO_3/CaO sorbent, which is not completely decomposed and regenerated to the K_2CO_3 at a temperature below 200 °C. Cho et al. prepared K_2CO_3-based sorbents using metal silicates as a support.[93] These sorbents exhibited an excellent regeneration ratio (>90%) with high CO_2 capture capacities at a low regeneration temperature of 200 °C compared to K_2CO_3-based sorbents using a metal oxide (Al_2O_3, CaO, SiO_2). Several studies identified that sufficient concentration of water plays a vital role in preventing the active species ($K_2CO_3{\cdot}1.5H_2O$) from converting to the original phase (K_2CO_3) in the carbonation step,[94,95] which is also confirmed by combining density functional theory (DFT) and phonon lattice dynamics by Duan et al.[96]

2.1.2. Intermediate Temperature. Intermediate temperature CO_2 capture sorbents such as MgO and Mg−Al layered double hydroxide (LDH) materials have been widely investigated in both the pre- and postcombustion CO_2 capture technologies in temperatures between 200 and 400 °C.[66] MgO has been considered a promising CO_2 capture sorbent because of its high theoretical CO_2 capture capacity (24.8 mmol CO_2/g sorbents), abundance, low cost, nontoxicity, and wide operation temperature (from room temperature to intermediate temperature).[97] CO_2 is captured by MgO through chemisorption to produce

https://doi.org/10.1021/acscatal.2c01646
ACS Catal. 2022, 12, 7486−7510

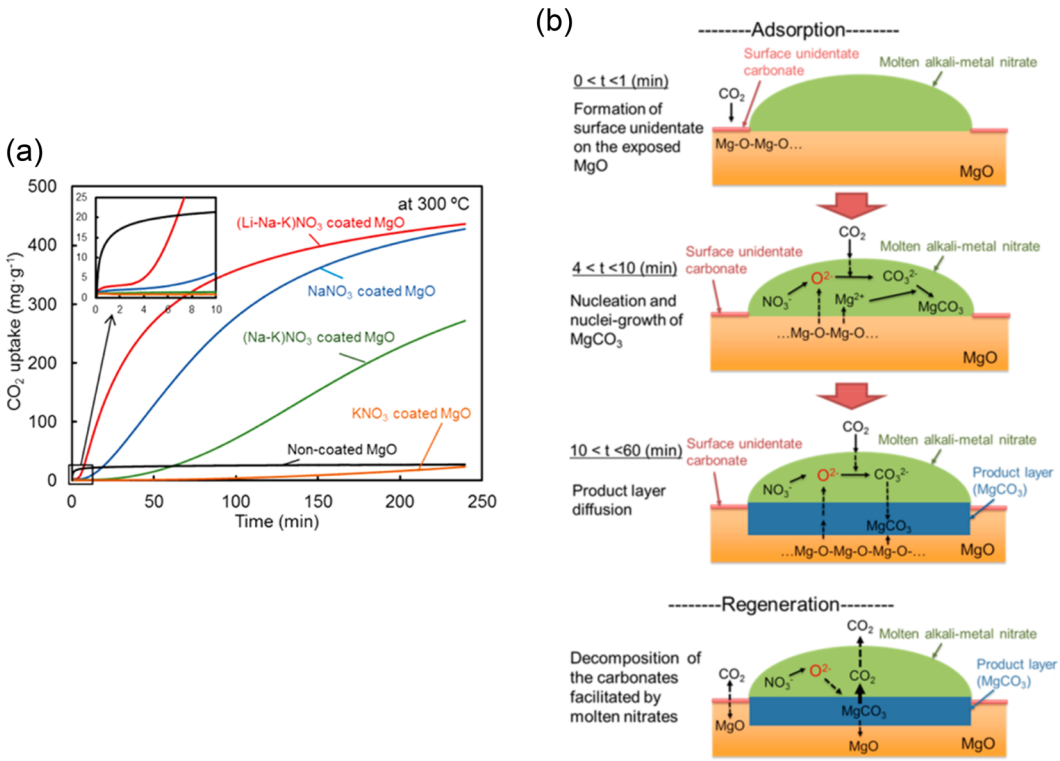

Figure 4. (a) Addition of alkali nitrates to MgO improved the CO_2 capture uptake of the composite material. (b) Schematic of the proposed adsorption and regeneration of molten-salt modified MgO that helps facilitate the capture and release of CO_3^{2-}. Reproduced from Reference 103. Copyright 2015, American Chemical Society.

$MgCO_3$ ($MgO + CO_2 \leftrightarrow MgCO_3$). However, a limited number of basic sites are exposed for CO_2 sorption because of its low specific surface area, resulting in poor CO_2 capture kinetics and capacity.[98,99] Moreover, MgO has a high sintering-rate after each thermal cycle, and the bulk volume expansion from the formation of $MgCO_3$ layer decreases the mass transport of CO_2 gas to the adjacent basic sites.[98]

Compared to other modification methods, molten salts-modified MgO-based sorbents have been widely applied to enhance CO_2 capture performance, regenerability of sorbents, and thermal stability.[100−102] Harada et al. reported effects of molten alkali metal nitrate modification of MgO-based sorbents on CO_2 capture capacity and regenerable properties.[103] The study suggested the presence of a high concentration of oxide ions in the molten alkali metal nitrates restricted the formation of rigid surface layers of unidentate carbonate and facilitated the generation of carbonate ions (CO_3^{2-}), resulting in the rapid formation of $MgCO_3$, increase in CO_2 uptake (Figure 4a), and ease of regeneration of the MgO-based sorbents (Figure 4b). Zhao et al. studied the effects of hydrothermal solution pH and metal promoters such as $NaNO_3$ and $NaNO_2$ over MgO-based sorbents to determine the optimal synthesis conditions.[102] The addition of $NaNO_2$ and $NaNO_3$ to MgO exhibited higher CO_2 capture capacity than the solely promoted-$NaNO_3$-MgO-based sorbents. Among these sorbents, the MgO-0.07$NaNO_3$-0.04$NaNO_2$ exhibited the highest CO_2 capture capacity of 19.0 mmol/g, equal to a MgO conversion of ∼96%.

LDH-based mixed metal oxides (MMOs) have been widely investigated because of their physicochemical properties.[104−106] LDHs are represented by the general formula $[M_{2+1-x}M_{3+x}(OH)_2]_{x+(A-x/n)}yH_2O$, where M_{2+} = Mg, CO, Ni, Ca, or Zn, M^{3+} Al, Fe, or Ga, A = anion (organic or inorganic ions), $0.15 \geq x \leq 0.33$ and $0.5 \geq y \leq 1.0$.[104,105,107] LDH-derived MMOs have been considered as ideal candidate materials for intermediate temperature CO_2 sorbents because of their fast sorption/desorption kinetics, high theoretical CO_2 capture capacity, ease of preparation, and low cost.[106] Manohara et al. synthesized LDHs with a mixed morphology using a modified amide hydrolysis method.[105] Acetate intercalated Mg−Al LDHs with two different Mg/Al ratios (3 and 4) were prepared by altering the starting precursors, synthesis method, and hydrolyzing agent. The acetamide acts both as a pH regulator and source of acetate ions, resulting in a new mixed morphology having both fibrous and sheet-like crystallites. These MMOs with high specific surface areas (316−341 m^2/g) exhibited an enhanced CO_2 capture capacity. They also utilized aqueous exfoliation coupled with the freeze-drying technique to develop LDHs-based novel MMOs and pelletized exfoliated LDH nanosheets for implementation in industrial-scale applications.[106] Mechanical characterization data exhibited a promising load-bearing capability and compressive strength of such pelletized samples. The exfoliated MMOs pellets showed improved cycling stability and excellent CO_2 capture capacity.

2.1.3. High Temperature. Two types of high-temperature CO_2 sorbents have been widely investigated, including CaO-based and lithium ceramics-based sorbents. These high-temperature CO_2 sorbents can be used for separating CO_2 in flue gas from fossil-fired power plants (postcombustion process) or syngas from hydrogen production (precombustion process). Calcium looping (CaL) technology is considered an efficient technology for separating CO_2 utilizing CaO-based solid sorbents because calcium minerals are one of the most abundant materials in nature (limestone or dolomite), and its high theoretical CO_2 capture capacity (786 mg CO_2/g sorbent or

https://doi.org/10.1021/acscatal.2c01646
ACS Catal. 2022, 12, 7486−7510

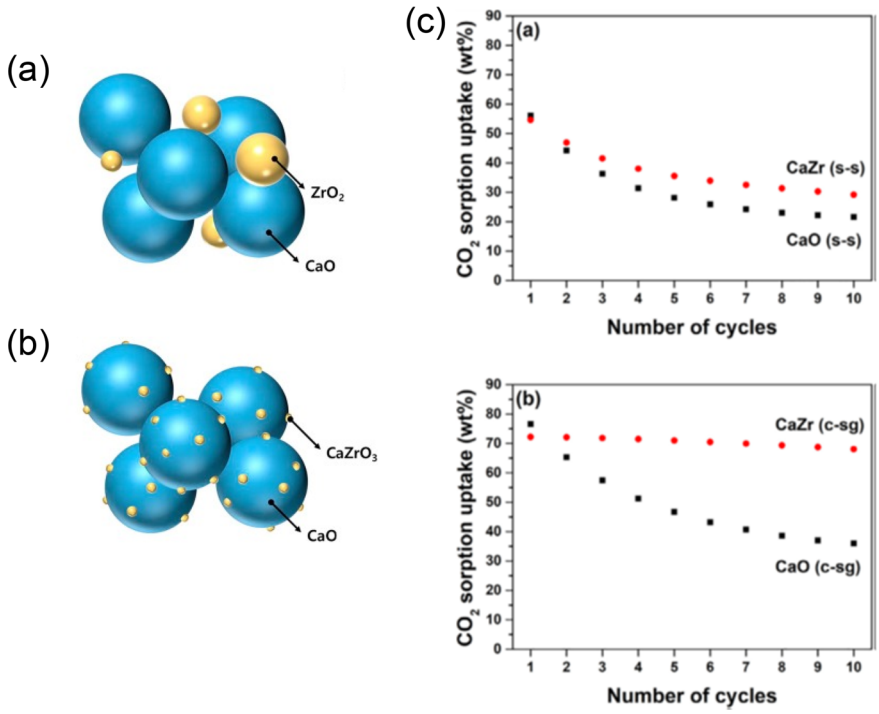

Figure 5. (a) Schematic of the CaZr sorbents prepared by the (a) solid-state method and (b) sol−gel method. (b) Comparison of the uptake capability of CaZr sorbents showing the superiority of the sol−gel synthesis method in forming improved CO_2 capture materials compared to the solid-state synthesized materials. Reproduced with permission from Reference 112. Copyright 2019, Elsevier.

17.8 mmol CO_2/g sorbents) through the following equations: $CaO(s) + CO_2(g) = CaCO_3(s)$.[108,109] A new concept for CO_2 capture from the iron and steel industry has been reported to exploit the inherent potential of the industry to produce lime in a CaL lime production, resulting in a significant reduction in the CO_2 avoidance cost.[110] The CaL process is a promising technology that has led to a reduction in CO_2 emission targets, increases in the degree of energy utilization, and minor additional costs.[111] CO_2 capture on CaO-based sorbents has been reported to occur via two processes: (1) fast chemisorption onto the CaO surface without any interruption, resulting in the formation of a thick layer of $CaCO_3$ covering unreacted CaO, and (2) slow diffusion of CO_2 through a thick layer of $CaCO_3$, followed by additional carbonation with the inner unreacted CaO phase.[109,112] However, during the CaL process, thermal sintering occurs under severe CaL conditions (carbonation, 650 °C; decarbonation, 950 °C) because this process is operated at a temperature higher than the Tammann temperature of $CaCO_3$ (∼533 °C). The reaction surface area of the sorbents reduces as the $CaO/CaCO_3$ crystallites and grains are repeatedly exposed to severe conditions in a cyclic system, resulting in its gradual decreases in CO_2 capture capacity.

Many researchers have studied various methods such as developing a preparation of CaO with high surface area, incorporating metal oxides into CaO, and surface modification to improve the textural properties and sinter-resistance of CaO-based sorbents.[113] Incorporating CaO into various thermally stable and inert supports has been widely investigated to solve the problem mentioned above.[109,113,114] Hu et al. thoroughly reviewed the research progress of incorporating CaO into various inert solid supports using different synthesis methods to enhance sintering resistance.[115] However, the major limitation of incorporating inert materials using the solid-state method and coprecipitation is that the structural properties of such a CaO sorbent cannot easily be tailored and effectively cover the sorbent.[112] Therefore, CaO-based sorbents with an excessive amount of inert materials synthesized using the solid-state method did not show a noticeable enhancement of the cyclic stability and had a very low CO_2 capture capacity. Lee et al. reported that CaO sorbents with a small amount of ZrO_2 (chemically attached to CaO) prepared by the sol−gel method showed much smaller particle size than those prepared using the solid-state method, resulting in enhanced CO_2 capture kinetics and capacity. They compare the CO_2 sorption kinetics of CaO-based sorbent quantitatively using the experimental data obtained from thermogravimetric analysis (TGA).[112] The TGA curves are fitted to the double exponential model to compare quantitatively CO_2 capture kinetics (eq 1).

$$y = Ae^{-k_1x} + Be^{-k_2x} + C \quad (1)$$

where y represents the weight percent increase of sorbents after CO_2 capture; k_1 and k_2 denote two exponential factors for (1) fast chemisorption and (2) slow CO_2 diffusion through the carbonate layer, respectively. A, B, and C are the pre-exponential factors.[112,116] Moreover, the chemically bonded Zr in CaZr sorbents prepared by sol−gel formed a mixed metal composite material with a CaO surface where ZrO_2 was well-dispersed. The close interaction of the ZrO_2 with the CaO grains increased the cyclic CO_2 capture stability and uptake by improving the sinter-resistance of the materials (Figure 5).

Hydration of the spent sorbent used for CO_2 capture in multiple cycles is one possible approach for sorbent reactivation in the following reaction: $CaO(s) + H_2O(g) \leftrightarrow Ca(OH)_2(s)$. During the hydration of CaO, the weak mechanical strength of $Ca(OH)_2$ causes cracks in the particle, thereby opening pathways for direct water penetration into the bulk unreacted CaO.[117] Moreover, it is reported that carbonation of $Ca(OH)_2$ is much faster than that of CaO. Despite the enhancement of

https://doi.org/10.1021/acscatal.2c01646
ACS Catal. 2022, 12, 7486−7510

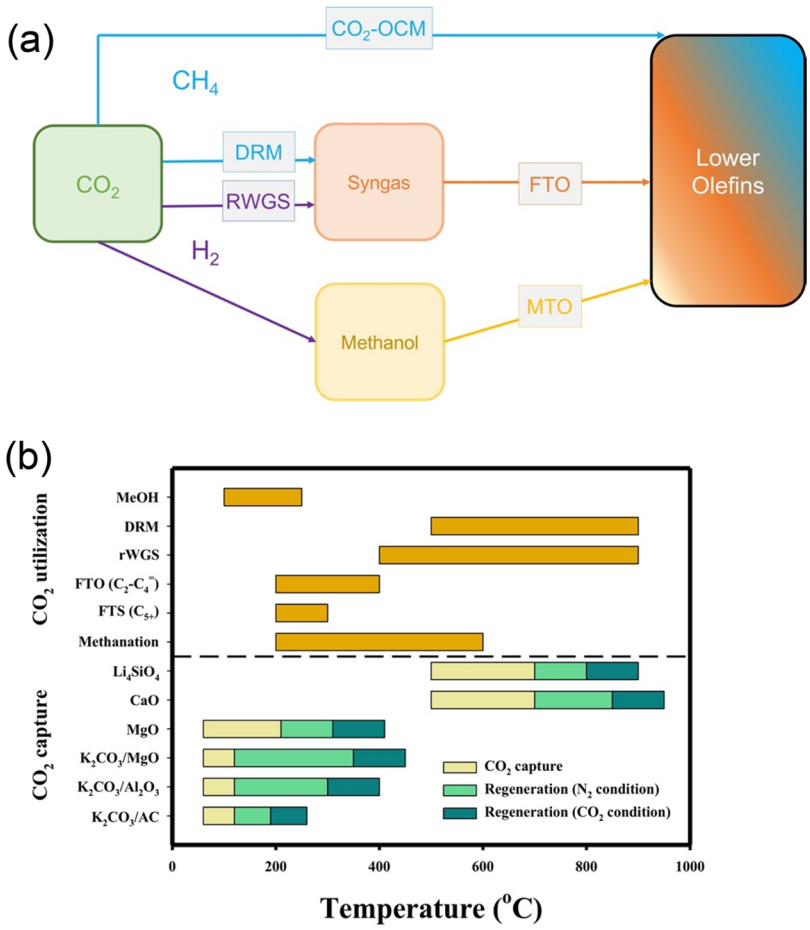

Figure 6. (a) Schematic of the reaction pathways for CO_2 utilization with renewable hydrogen to olefins. (b) Table of sorbent properties (discussed in section 2) and the CO_2 utilization temperature ranges.

CO_2 capture capacity after hydration, the use of steam will raise the total cost for sorbent-based CO_2 capture technology.

Attrition of the CaO-based sorbents during the carbonation and calcination in multiple cycles is a great concern. In the CaL, the CaO-based sorbents continuously circulate between the fluidized-bed carbonation and the calcination reactors. Jia et al. studied attrition tests in a fluidized bed reactor using calcining limestone beds, suggesting that multiple carbonation/calcination cycles result in severe fragmentation during the first or two calcination periods.[118] Among the possible binders for pelletization of CaO-based sorbents, calcium aluminate cement (CAC) has been widely used for pelletization because of its fast setting, good refractory properties, and inexpensive cost.[119] Chen et al. reported that the mechanical properties of the CaO pellet with CAC were greatly enhanced, inproving CO_2 uptake and showing slow decay in CO_2 capture capacity during multiple cycles.[120] They also found that the order of effects of parameters on attrition was temperature > superficial gas velocity > exposure time > pressure.

Many lithium containing ceramics (Li_4SiO_4, Li_8SiO_6, Li_2ZrO_3, Li_5AlO_4, $LiFeO_2$, and Li_2CuO_2) have been developed for the high-temperature CO_2 sorbents because of their relatively high theoretical CO_2 capture capacity, compared to other alkali metal-containing ceramics.[121] Namely, lithium orthosilicate (Li_4SiO_4) has been widely investigated among the many other lithium containing ceramics because of its higher CO_2 sorption capacity, cyclic stability than $LiFeO_2$, Li_2CuO_2, and Li_8SiO_6, and lower cost than Li_2ZrO_3.[121,122] Moreover, the decarbonation temperature of Li_4SiO_4 sorbents is much lower than that of CaO-based sorbents among the high-temperature CO_2 sorbents, leading to lower energy consumption for the decarbonation of sorbents.[122] Recently, many researchers have been trying to use cheap raw materials such as cheap Si resources from industrial solid wastes or minerals because the cost of lithium containing ceramics is expensive in comparison to CaO-based sorbents.[121,123,124] The basic reversible reaction for CO_2 sorption by Li_4SiO_4 material has been widely reported: $Li_4SiO_4(s) + CO_2(g) \leftrightarrow Li_2SiO_3(s) + Li_2CO_3(g)$.[121,122] The double-shell mechanism is regarded as the most appropriate model for the reaction occurring between Li_4SiO_4 and CO_2 in two stages.[122,125] In the first stage, CO_2 molecules react with Li_4SiO_4 particles on the surface of sorbents without interruption, leading to the formation of a double shell composed of Li_2CO_3 and Li_2SiO_3 covering the internal Li_4SiO_4. Then, the CO_2 and Li^+ diffuse through the external double-shell; meanwhile, the thickness of the double-shell increases as the reaction proceeds. Thus, the second stage is much slower than the first stage due to the high diffusion resistance of the CO_2.

Li_4SiO_4 sorbents were prepared using various Li precursors (Li_2CO_3, LiOH, and $LiNO_3$) and silica (quartz, silica gel, fumed silica, and colloidal silica). Most of the Li_4SiO_4 materials were prepared using Li_2CO_3 and SiO_2 by the conventional solid-state reaction method at a relatively high temperature above 720 °C to obtain a pure Li_4SiO_4 phase leading to the formation of nonporous and low surface area Li_4SiO_4 sorbents.[122] The bulk framework of Li_4SiO_4 does not effectively capture CO_2 because

https://doi.org/10.1021/acscatal.2c01646
ACS Catal. 2022, 12, 7486−7510

of the very slow diffusion of CO_2 and Li^+. Various strategies have been investigated to enhance the CO2 capture performance by promoting CO_2 diffusion or preventing sintering by adding K and Na salts to form eutectic or metal doping to produce defects.[126−128] Kwon et al. prepared the lithium silicate-based sorbents by a solid-state method using Li_2CO_3 and colloidal silica with different Li/Si molar ratio (2, 3, 3.6, and 4), producing different amounts of Li_4SiO_4 and Li_2CO_3 phases and different crystallite size of Li_4SiO_4.[129,130] The presence of Li_2CO_3, act as a physical barrier, prevent sintering of Li_4SiO_4 in the sorbent. They also found that lithium silicate-based sorbent with Al_2O_3 showed a much faster CO_2 sorption ration and relatively stable CO_2 capture capacity during 55 cycles.[130] Kim et al. synthesized microporous Li_4SiO_4 by a simple solid-state method using LiOH and fumed silica.[131] The pure Li_4SiO_4 with a microporous structure formed at relatively low temperature when LiOH is used as a precursor, compared to Li_4SiO_4 using Li_2CO_3 and $LiNO_3$. The microporous Li_4SiO_4 dramatically enhanced CO_2 capture performance (capacity and kinetics) at 550 °C and multicycle stability during 10 cycles. Subha et al. prepared platelet-shaped Li_4SiO_4 particles by a sol−gel approach employing the $LiNO_3$ and colloidal silica, exhibiting considerably higher CO_2 capture capacity and faster CO_2 sorption rate than those prepared by the solid-state method.[132] In addition, a porous carbon mesh coated with sol−gel-based particles exhibited a CO_2 capture capacity of 150 mg/g and a CO_2 sorption rate of 37.5 mg/g/min with stable carbonation and decarbonation performances for 8 cycles. Belgamwar et al. synthesized lithium silicate nanosheets (LSNs) by solid-state thermal treatment of $LiNO_3$ and dendritic fibrous nanosilica with a Li/Si molar ratio of 4.66.[125] Because of the nanosheet morphology of the LSNs, the sorbents exhibited a good external surface for CO_2 adsorption at every Li-site, yielding an excellent CO_2 capture capacity close to the theoretical maximum value and extremely fast CO_2 capture kinetics. In addition, the LSNs showed dramatic stability without any loss in the CO_2 capture capacity and kinetics even after 200 cycles. They also proposed a mechanism of the mixed-phase model to explain the unique CO_2 capture performances of LSNs.

3. CO_2 UTILIZATION FOR HYDROCARBON AND LOWER OLEFIN PRODUCTION

The primary chemical process for olefin production is the use of thermal steam cracking. Naptha is currently the predominant feedstock for steam cracking. The light olefins produced, such as ethylene and propylene, are used as building blocks for chemicals, polymers, and fuels.[133] Steam cracking (SC), also known as thermal pyrolysis, is currently the leading method for olefin production of ethylene and propylene and uses different types of hydrocarbons as feedstock, from natural gas liquids to petroleum liquids.[134] Deep catalytic cracking (DCC) was also developed to utilize all parts of petroleum to increase the production of light olefins from heavy oil feedstock.[135] The processing strategies, as mentioned above, heavily rely on a petroleum-based feedstock to produce olefins and generate significant CO_2 emissions. The increasing demand for these products and the need to move away from petroleum have spurned investment and research in alternative feedstocks, including coal, natural gas, biomass, waste stream, and derivatives.[136] Among the most promising is the use of CO_2 and renewable H_2 to form indirect and direct pathways to olefins using processes such as methanol to olefins (MTO), methanol to propylene (MTP), oxidative coupling of methane (OCM), and Fischer−Tropsch synthesis to olefins (FTO). This section will describe the different pathways to produce synthesis gas or direct conversion of CO_2 to form C_1 and lower olefin products (Figure 6a). Section 4 will discuss the coupling of the sorbents discussed in section 2 with properties conducive to subsequent CO_2 conversion (Figure 6b).

3.1. Indirect Conversion to Lower Olefins. *3.1.1. CO_2 to Synthesis Gas: Reverse Water−Gas Shift.* One of the more mature reaction pathways for CO_2 conversion is the formation of carbon monoxide through the reverse water−gas shift (RWGS) reaction. Depending on the reaction conditions, the hydrogenation of CO_2 can produce CO ($CO_2 + H_2 \rightarrow CO + H_2O$) or CH_4 ($CO_2 + 4H_2 \rightarrow CH_4 + 2H_2O$). Typically, CO formation is thermodynamically favorable at high temperatures, while the dominant product is CH_4 at lower temperatures. The CO conversion process has been studied because of the well-established processes to further convert CO into other fuels and alcohols using either the Fischer−Tropsch process or methanol synthesis.

The elementary steps for RWGS reaction include the following: (1) adsorption of CO_2 and dissociation of one of the C═O bonds, and (2) dissociation of H_2 to hydrogenate oxygen to form H_2O. To favor CO production, the metal catalyst needs to have mild C═O dissociation to avoid complete dissociation of CO and prevent further hydrogenation of the CO to methane and methanol. Generally, the most common catalysts used for RWGS include noble metals such as Rh, Ru, Pt, Pd, Ir, and Au, transition metals like Ni, Fe, and Cu, and mixed metal oxides.[137−140] For example, Pt and Pd have a high hydrogenation ability to produce CO. In contrast, Ru, Cu, and Rh have a strong C═O breaking ability and are more selective in producing CH_4 because they are mildly oxophilic.[141] The RWGS with mixed metal oxides either occur via a redox pathway where adsorbed hydrogen produces oxygen vacancies to activate CO_2 or an associative mechanism where adsorbed CO_2 reacts with dissociated hydrogen to form intermediate species that decompose into the final products.[139]

The interaction between the support and the metal catalyst is important for tuning the selectivity and activity of the RWGS reaction. The reducibility and acid−basic properties of the supports can influence CO_2 adsorption and activation. There are two types of supports: irreducible (SiO_2, Al_2O_3) and reducible (TiO_2 and CeO_2). The irreducible supports do not directly activate CO_2; however, they facilitate CO_2 adsorption at the interface of the metal support. For example, Kattel et al. showed through DFT calculations that when Pt is supported to SiO_2, the CO_2 adsorbs at the interface of the support and metal.[142] Reducible supports like TiO_2, and CeO_2, typically generate oxygen vacancies which allow for the strong adsorption and activation of CO_2. Supports with acidic characteristics typically have higher activity and selectivity to CO for the RWGS reaction. Sakurai et al. observed CO_2 hydrogenation of Au on three different supports (CeO_2, ZrO_2, and TiO_2).[143] Their studies showed that they all have identical CO selectivity, but there was higher activity using the Au/TiO_2 samples due to the higher acidity of TiO_2 compared to ZrO_2 and CeO_2. CH_4 selectivity is higher on reducible supports because the O atoms are removed from CO_2 due to the oxygen vacancies, and hydrogenation occurs on the C species.[144] Unfortunately, one of the primary deactivation mechanisms for supported metal catalysts is the accumulation of carbon species.

For some catalysts, the RWGS reaction occurs at the support and the metal interface. Maximizing the metal surface area or the

https://doi.org/10.1021/acscatal.2c01646
ACS Catal. 2022, 12, 7486−7510

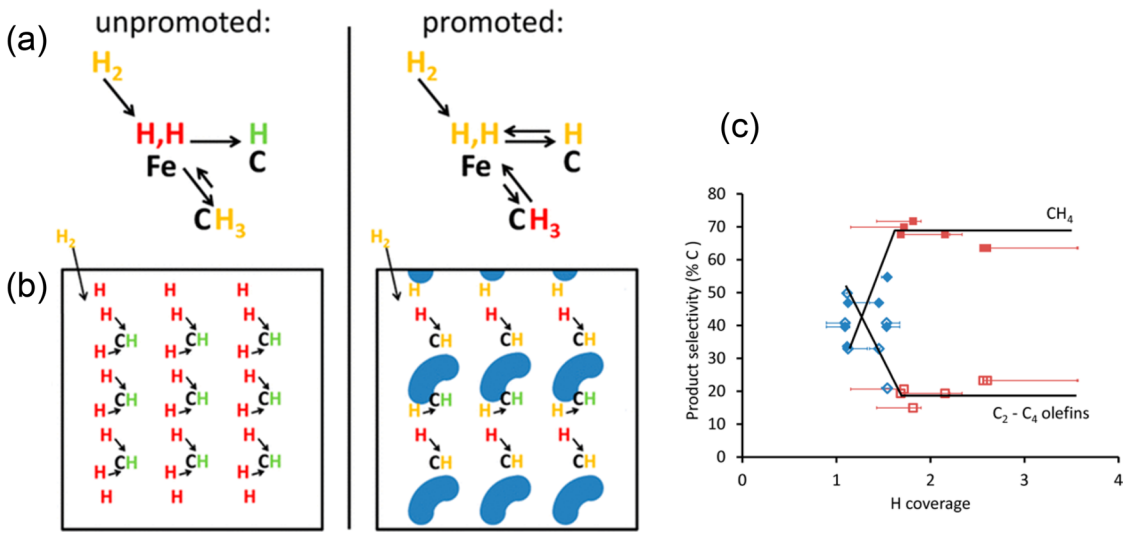

Figure 7. Cartoon of promoter effect by Na_2S. Colors of hydrogen atoms denote their energy: red, yellow, and green denote high, medium, and low energy, respectively. The blue shapes denote the Na_2S species. (a) The promoter increases the H adsorption strength on iron and decreases the adsorption on carbon, thereby decreasing methane formation and increasing olefin formation. (b) The strength of the effect differs per site, but at both sites the equilibrium between binding to iron or carbon is shifted. (c) Product selectivity as a function of H coverage (350 °C, 1.85 bar, $H_2/CO = 10$): blue ◆ CH_4 and blue ◇, C_2-C_4 olefins selectivity for promoted catalysts; red ■ CH_4 and red □, C_2-C_4 olefins selectivity for unpromoted catalysts. Reproduced from Reference 152. Copyright 2016, American Chemical Society.

number of metal-interface sites is critical to its performance. This can be achieved by reducing the metal particle size. Depending on the size of the metal particle and the interface of the metal to the support, the dominant product of the same material can be shifted. For example, Atibekova et al. synthesized 2.6 nm Ru particles dispersed on three different supports (TiO_2, CeO_2, and Al_2O_3).[145] They found that the reducible supports were more active than Al_2O_3, but CH_4 was the main product. Atomically dispersed RuO_x formed sites on the CeO_2 supports changed the main product to CO attributing to the weakened CO adsorption on the RuO_x sites.

The catalytic conversion of CO_2 to CO via the RWGS reaction can be a way to convert CO_2 into valuable chemicals and fuels. Key challenges for these reactions area are due to the catalytic material's low-temperature activity and selectivity. Enhancing CO_2 adsorption and facilitating CO desorption are key factors for enhancing CO_2 conversion and CO selectivity. Varying the supports characteristics and tuning the metal–support interaction can provide additional strategies to help improve the selectivity and activity of the materials.

3.1.2. Reverse Water–Gas Shift and Fischer–Tropsch Reaction. The FT process is a catalytic polymerization reaction for the conversion of synthesis gas into a variety of products like alkanes (paraffins), alkenes (olefins), and cycloalkanes (naphthenes) that can be refined into synthetic fuels, lubricants, and petrochemicals by CO polymerization and hydrogenation on a metal catalyst. Light olefins are key building blocks in the chemical industry, and they are essential chemicals used to fabricate synthetic rubbers, solvents, plastics, and cosmetics.[32] Typically, the syngas, which consists of a mixture of CO_2, H_2, CO, and H_2O used as the feed in FT is made by the RWGS reaction.[146,147]

Davis and de Smit et al. have explored Fischer–Tropsch mechanisms.[146,147] Although there are several possible mechanisms for FT, the overall process is like a general polymerization reaction that involves reactant adsorption, chain initiation, chain growth, propagation, and termination. Initiation occurs after the CO is adsorbed on the FT catalyst and becomes the chain initiator by dissociating and hydrogenating. The chain growth or the propagation step occurs by adding CO to the chain initiator or an already growing chain on the catalyst surface. The growth mechanism for hydrocarbons on the metal catalyst is the surface carbide mechanism by CH_2 insertion.[148] This mechanism is first initiated by the metal surface adsorbing carbon monoxide and dissociating it to form carbide and oxygen species. Hydrogen is also adsorbed and dissociated on the metal catalyst. The carbon atoms are then hydrogenated to form CH_2, and oxygen is removed as water. The termination step determines the length of the chain and the terminating functional group. It is influenced by the nature of the catalyst and the operating conditions. Two specific processes for termination are thermal desorption and reactive desorption. Thermal desorption is caused by the growing chains weakening the bond between the catalyst and the surface intermediate. Reactive desorption is the desorption by breaking the bonds between the catalyst and the surface intermediate.

Typical FT catalysts are group VIII metals and platinum group noble metals like Fe, Co, Ni, Ru, and Rh. The most active catalysts for FT synthesis are Fe, Co, Ni, and Ru. Iron and cobalt catalysts are the most commercially used because they are inexpensive and abundant compared to other active metals.[149] In addition, Fe- based catalysts have been widely used for their high activity for both RWGS and FT synthesis and resistance to sulfur poisoning.[147] Cobalt catalysts give the highest yields and the longest lifetime and produce linear alkanes.[150] Nickel is not as commonly used because it produces more methane and forms volatile carbonyls at the FT reaction conditions, resulting in a continuous metal loss and a shorter activity lifetime. Ruthenium, although highly active, is expensive to mass produce. The activity of FT catalysts is dependent on H_2 adsorption and the ability to adsorb and dissociate CO. and are based on the reducibility of their oxides. Cobalt, nickel, and ruthenium remain in their metallic states during FT conditions, while iron-based catalysts are prone to phase changes.

The main deactivation causes for FT catalysts are surface fouling, oxidation of the catalyst, and sintering. The surface

https://doi.org/10.1021/acscatal.2c01646
ACS Catal. 2022, 12, 7486−7510

fouling or deposits can be removed by hydrogenation or washing with a light hydrocarbon liquid. In the case of Fe catalysts, deactivation can occur when oxidized and water is present. The two main strategies that have been used to improve the catalytic performance of catalysts are to increase the number of active sites on the catalyst or to increase the intrinsic activity of each active site.[32] This has been explored by adding promoters to the metal catalysts, support effects, using bimetallic alloys, or encapsulation of the metal catalyst.

The addition of promoters to FT catalysts can increase light olefin yields by controlling the electronic and structural properties.[151] The addition of promoters can improve lower olefin selectivity of iron-based catalysts such as alkali metals.[149] Sodium has been studied as a promoter for iron catalysts because it increases the chain growth probability and enhances olefins production. Researchers have used alkali metal promoters in Fe-based catalysts, which promote the growth of hydrocarbon chains by weakening their affinity with H_2 while enhancing the adsorption strength of CO_2 and CO.[32] Xie et al. studied the effects of Na and S promoters on Fe catalysts showing that the Na_2S promoters increase the H adsorption strength on iron and decrease the adsorption of carbon, increasing olefin production by decreasing methane formation (Figure 7).[152] Cheng et al. showed the effects of sodium on Fe catalysts supported by reduced graphene oxide (rGO). The addition of Na increased the basicity of the Fe surface which improved the chain growth probability and reduced methane formation. It increased the adsorption capacities of CO and H_2, increasing the overall activity and selectivity of this material.[153] Ma et al. researched the effects of Na promoters on Fe−Zr catalysts. They showed that Na had a strong electron transfer from Na to Fe, which caused the electron-rich iron species to dissociative to adsorb CO and hydrogen, resulting in enhanced chain propagation and a decrease in the hydrogenation of light olefins, increasing olefin selectivity.[154] Rare earth metals have also been shown to be good promoters for Fe-based catalysts. Han et al. studied rare earth metal promoters on Fe-based catalysts. Nd promoted Fe catalysts showed dissociated adsorption of CO due to the electron transfer between Nd and Fe, which contributed to increasing the surface charge density of iron atoms. Nd also enhanced the catalysts' surface basicity and inhibited the hydrogenation reaction, resulting in high light olefin production.[155]

Researchers have tried to improve catalytic performance by using bimetallic systems, including Co−Fe,[156] Fe−Mn, Fe−Ni, and Co−Ni.[157] Supported catalysts have also been used to maximize the surface area of the active phase. These include silica, alumina, and zeolite-supported catalysts. Encapsulation is another strategy that has been used for improved catalytic activity and lifetime by having strong thermal stability against sintering.[158] The encapsulation strategies consist of core−shell, core−tube, mesoporous, and lamellar structures. The binding energy between metal nanoparticles and reactive molecules can be tuned with the presence of encapsulation structures. Encapsulation decreases catalyst particle interaction, which decreases sintering.

The catalytic hydrogenation process can mitigate CO_2 emissions and be used for olefin production. FT is a well-established process that has been commercially established and can be paired with the RWGS reaction. It is important to understand the material properties to optimize and tailor the FT reaction toward the desired product. Fe- and Co-based catalysts have been extensively studied due to their low cost and high activity. Adding promoters, using bimetallic alloy systems, incorporating support effects and encapsulation are strategies that have been explored to improve catalyst activity, selectivity, and overall lifetime of the material.

3.1.3. Dry Methane Reforming. Dry methane reforming (DRM) is an endothermic reaction that converts CH_4 and CO_2 into synthesis gas (H_2 and CO), typically on an active metal catalyst.[159] The H_2/CO ratio for DRM is typically 1. It is an endothermic reaction because it requires the breakdown of very stable molecules and requires high operating temperatures. The mechanism for DRM involves the adsorption and dissociation of CH_4 and CO_2 as well as hydroxyl group formation. The dissociation of methane is the rate-determining step. CO_2 and CH_4 adsorption, dissociation, and reduction are dependent on the catalyst properties. CO_2 typically adsorbs on the metal−support interface and can occur via C- and O-coordination or a mixture of both.[160] The development of highly active and stable catalysts with resistance against deactivation is important factors to consider for the successful wide-scale implementation of DRM.[161] Catalytic activity and stability are influenced by active metal dispersion, metal−support interaction, resistance to sintering, and low carbon formation.

Typical DRM catalyst materials include noble metals (Ru, Rh, Pt, Pd, Ir) and non-noble (Ni, Co) metal catalysts. Noble metals are highly active and are resistant to carbon formation but are not widely used due to their high cost and limited availability.[162] Transition metals such as Ni and Co have been widely used in DRM due to their high activity, low cost, and wide availability. However, they tend to have fast deactivation due to carbon formation limiting their usability and reducing their overall lifetime.[163−166] Hou et al. investigated the effect of noble metals like Rh, Ru, Pt, Pd, and Ir supported on mesoporous Al_2O_3 and compared it to inexpensive Ni and Co. They showed that noble metals have higher coke resistance, but their overall activity was lower when compared to Ni and Co.[162]

Several strategies have been investigated to circumvent deactivation by carbon formation using either a promoter, support effects, changing the metal particle size, or using bimetallic alloys.[167] Choosing an ideal support can enhance the metal−support interaction, which can reduce metal sintering. Supports not only prevent sintering and increases metal dispersion, but they take part in the DRM reaction. The metal−support interaction can affect the stability and reducibility of the catalyst by providing physicochemical properties such as basicity, oxygen storage capacity, and reducibility.[168] Zhang et al. investigated the effects of supports like SiO_2, TiO_2, Al_2O_3, MgO, and ZrO_2 on the catalytic performance of Ni.[169] They showed that a mix of Al_2O_3−MgO support had the highest catalytic activity. Studies showed that having high dispersion, high surface area, and small particle size contributed to higher activity and a more stable catalyst. Sokolov et al. studied Ni catalysts supported on Al_2O_3, MgO, TiO_2, SiO_2, ZrO_2, and La_2O_3−ZrO_2.[170] They showed that Zr-based supports showed the highest initial activities, and La_2O_3−ZrO_2 showed the highest stability. El Hassan et al. dispersed Co nanoparticles onto mesoporous silica (SBA-15), which strongly enhanced the stability and prevented the sintering of the Co catalyst. They also showed that adding Rh promoted the Co reducibility, enhanced the catalytic performance, and prevented coke formation.[171] Zhang et al. synthesized a highly stable Ni catalyst on SBA-15. They prevented the deactivation of the catalyst by limiting the sintering of Ni and having high dispersion throughout the support.[172]

https://doi.org/10.1021/acscatal.2c01646
ACS Catal. 2022, 12, 7486−7510

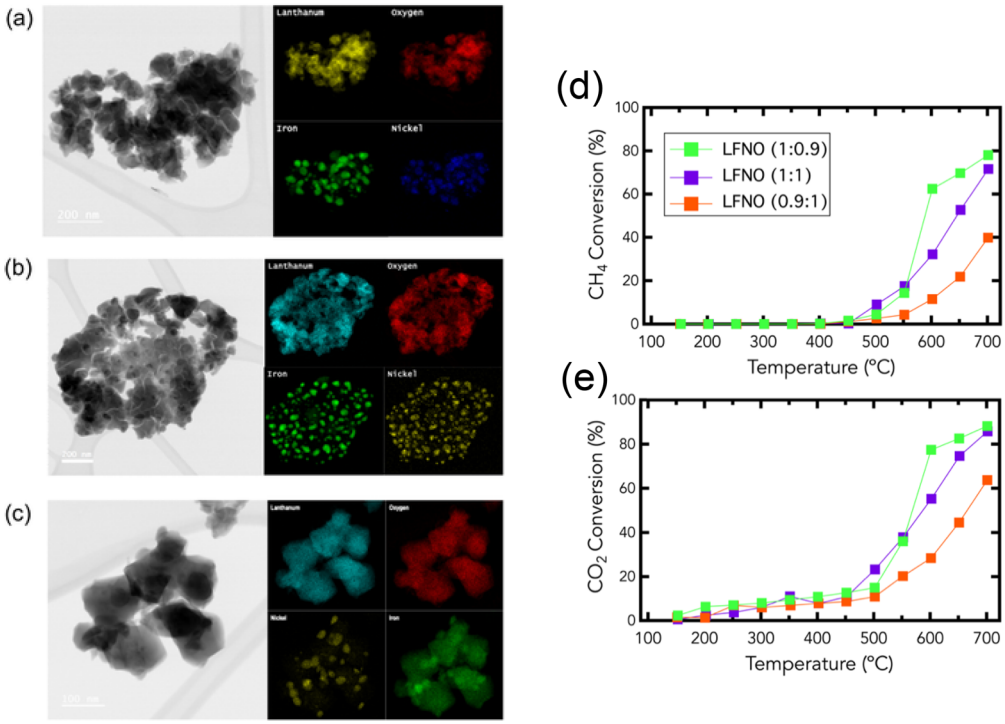

Figure 8. STEM-BF images of Ni−Fe nanoparticles exsolved from (a) $La_{0.9}FeNi_{0.1}O_3$ - LFNO(0.9:1), (b) $LaFe_{0.9}Ni_{0.1}O_3$ - LFNO(1:0.9), and (c) $LaFeNi_{0.1}O_3$ - LFNO(1:1). The respective (d) CH_4 conversion and (e) CO_2 conversion of the different Ni−Fe nanoparticles from different precursor systems. Reproduced with permission from Reference 181. Copyright 2020, John Wiley and Sons.

Studies have shown that acid−base properties of the support can affect the catalytic activity. The acidity of catalysts can inhibit the dissociative adsorption of CO_2 on the catalyst surface due to the increase of dehydrogenated carbon depositions deactivating the catalyst.[173] Das et al. investigated the SiO_2 and Al_2O_3 supports on Ni catalyst and developed a synergistic correlation between the acidic and basic properties of the support.[174] They revealed that having a large number of acid sites on the support deactivates the catalyst by coke formation. CO_2 is acidic, so basic supports like MgO can enhance the ability of CO_2 chemisorption and coke resistance.[175] A study by Gadalla and Bower showed that using commercial Ni catalysts on different supports, including γ-Al_2O_3, Al_2O_3−CaO, Al_2O_3−SiO_2, and Al_2O_3−MgO. The study determined that the best support overall was the Al_2O_3−CaO and Al_2O_3−MgO supports that had high conversion and stability due to the formation of intermediate species calcium aluminate or magnesium aluminate.[176]

Perovskite-type oxides have been used as catalyst precursors for DRM and suppress carbon formation on Ni-based catalysts.[177] Gallego et al. showed that using $LaNiO_3$ and La_2NiO_4 as catalyst precursors obtained high activity for carbon dioxide reforming of methane, with La_2NiO_4 showing the best performance. Using La_2NiO_4 led to the formation of small nickel particles of 7 nm, which was responsible for the higher catalytic activity.[178] Kawi et al. showed that $LaNiO_3$ had been successfully used as a crystalline catalyst precursor for methane reforming when compared to La_2O_3. $LaNiO_3$ can perform at higher temperatures to achieve CH_4 conversion without deactivating the Ni.[179] Arandiyan et al. compared the catalytic activity, stability, and surface properties of different perovskite-type oxides doped with different noble metals, and Rh showed the highest activity.[180] Our lab has explored perovskite type-oxides for forming metal alloys, Ni−Fe[181] and Ni−Fe−Co,[182] for the DRM reaction. Recent findings showed that the inherent defect material properties of the perovskite precursor influenced the composition and size of the Ni−Fe nanoparticles exsolved and the inherent catalyst performance and stability (Figure 8). The Ni−Fe nanoparticles exsolved from $LaFe_{0.9}Ni_{0.1}O_3$ showed the best catalyst performance and were regenerable after 24 h of aging.

Alloying Ni catalysts with Co was also shown to improve the overall performance of the catalysts. Zhang et al. studied different compositions of Ni−Co bimetallic catalysts. Synergistic effects of Ni and Co provided high activity, carbon formation resistance, and stability.[183] Hou et al. compared coke deposition resistance of Ni−Co alloys supported on alumina.[162] Wan-Ying et al. performed DFT calculations on DRM mechanisms of Ni and a Ni−Mo alloy. They showed that the activation of CH_4 and CO_2 is higher in the Ni−Mo compared to monometallic Ni.[184] Turap et al. tested a series of Co−Ni catalysts with different ratios.[185] The Co/Ni ratio of 0.8 showed the highest catalytic activity.

Promoters are used to modify the catalyst structure to improve stability or enhance the catalytic reaction to give better activity or selectivity.[186] Zeng et al. added natural rare earth metal oxide promoters (La_2O_3, CeO_2, Nd_2O_3, etc.) to Co catalysts supported on γ-Al_2O_3, enhancing the catalytic activity and stability of the catalyst.[187] The promoters decreased the size of the Co_3O_4 particles, enhanced the dispersion degree of the Co, and prevented sintering by strengthening the metal−support interaction. Jeong et al. investigated the catalytic activity of Ni/HY catalysts promoted by Mg, Mn, K, and Ca. The Mg promoted Ni/HY showed the highest carbon formation resistance and the most stable catalytic performance as no significant loss in performance was observed after 720h of reaction testing.[188] This can be attributed to the reduced Ni particle size caused by Mg promotion. San Jose-Alonso et al.

https://doi.org/10.1021/acscatal.2c01646
ACS Catal. 2022, 12, 7486−7510

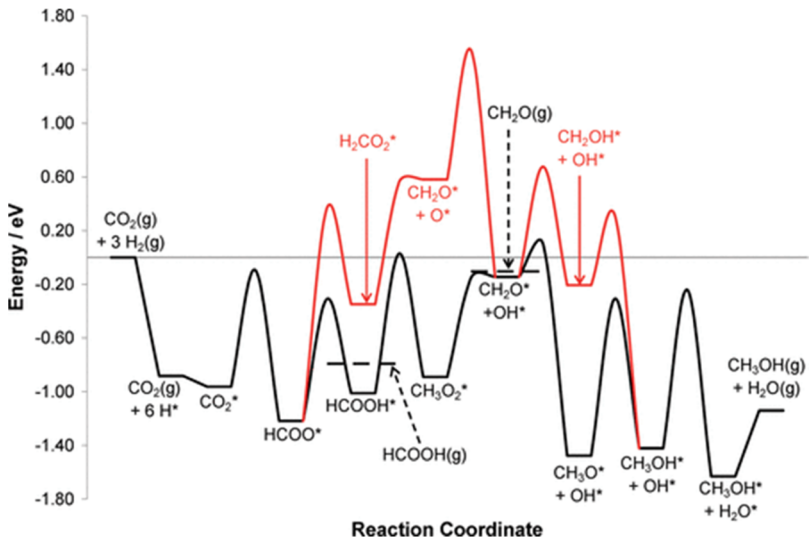

Figure 9. Potential energy surface of methanol synthesis via CO_2 hydrogenation. The black line indicates the lowest-energy pathway through the HCOO*, HCOOH*, CH_3O_2*, CH_2O*, and CH_3O* intermediates. The main intermediates along the red path are HCOO*, H_2CO_2*, CH_2O*, and CH_2OH*. The two dashed horizontal lines indicate the desorption barriers of HCOOH and CH_2O. Reproduced from Reference 193. Copyright 2011, American Chemical Society.

studied alumina-supported Co catalysts promoted by K and Sr. Both K and Sr showed similar catalytic activity, but K had lower carbon deposition. The addition of K reduced the catalytic activity due to the size of the Co particles being larger, reducing the number of active sites.[189]

3.1.4. CO_2 to Methanol. Methanol is a commonly used chemical for various applications like fuels and fuel additives used in feedstock production of small hydrocarbons.[190] Methanol can be produced from the synthesis gas derived from coal, natural gas, and other hydrocarbons.[191] The most established method for methanol production comes from the use of syngas (CO and H_2) which are then converted to methanol over a heterogeneous catalyst. Methanol synthesis from CO is a highly exothermic process and is thermodynamically favorable at low temperatures.[192] The most established and commercially used catalyst is $Cu/ZnO/Al_2O_3$.[193] However, there are still questions regarding the nature of the active sites and the reaction mechanisms.[194]

CO_2 hydrogenation to produce methanol has been increasing in research demand. Synthesis gas contains a significant amount of CO_2 that can also be hydrogenated from methanol. Grabow et al. performed DFT calculations on Cu surfaces of $Cu/ZnO/Al_2O_3$ for selective hydrogenation of CO_2. CO_2 is hydrogenated in the sequence $CO_2^* \rightarrow HCOO^* \rightarrow HCOOH^* \rightarrow CH_3O_2^* \rightarrow CH_2O^* \rightarrow CH_3O^* \rightarrow CH_3OH^*$, while CO hydrogenation to methanol is $CO^* \rightarrow HCO^* \rightarrow CH_2O^* \rightarrow CH_3O^* \rightarrow CH_3OH^*$.[193] An example of the calculated potential energy surface is shown in Figure 9, showing that the pathway that there are two energetic pathways for CO_2 hydrogenation. Ashwell et al. also performed a DFT calculation on Ni(110) metal surfaces to observe the theoretical yields on ethanol by CO hydrogenation.[195] They also found the H_3CO intermediate followed by a final hydrogenation step toward methanol. There are also efforts to develop non-Cu catalysts for methanol synthesis from CO_2. For instance, Docherty et al. showed that PdGa nanoparticles supported on Ga-doped silica supports had a high selectivity toward methanol that was much more selective than $Cu@ZrO_2$ and $Cu@SiO_2$.[196] Studies by Koizumi et al. showed that Pd supported on SiO_2 supports with promoters of K, Ca, and Mg enhanced their activity toward methanol synthesis.[197] An inverse catalyst of ZrO_2−Cu catalysts was doped with ZrO_2 and showed that an increase of the activity toward methanol was from the improved hydrogen activation and CO_2 activation ability.[198]

3.2. Direct Conversion to Lower Olefins. *3.2.1. CO_2 Oxidative Coupling of Methane (CO_2 to OCM).* The conventional OCM reaction scheme uses rare-earth oxides or carbonate catalysts to transform CH_4 and O_2 or CO_2 into ethane or ethylene.[199−202] The reaction is complex and involves homogeneous and heterogeneous reactions. Broadly, there are five kinds of catalyst−support systems that are active for this reaction: (1) pure, highly basic oxides including early lanthanide oxide (except ceria), (2) group IA and IIA metals supported on basic oxides such as Li/MgO, Ba/MgO, and Sr/La_2O_3, (3) monophasic oxides, (4) group IA metals supported on certain transition metal oxides, and (5) any of these materials with chloride promoters.[203] However, OCM has limited industrial implementation due to the poor selectivity of the C_2 products. The predominant dry reforming or partial oxidation is a competing reaction that can form the undesired product of CO and H_2.[204] Additionally, the formed ethane and ethylene can also become oxidized back into CO_2, lowering the overall yield. Nevertheless, OCM is an essential reaction for the direct utilization of CO_2 and CH_4 into ethane and ethylene, a valuable intermediate for the chemical industry.

There are several theories on the use of CO_2 for OCM. However, the most predominant one is that the CO_2 replenishes surface oxygen species of the mixed oxide catalysts that mediate heterolytic cleavage of methane. Yoon et al. cofed CO_2 and O_2 for OCM and observed an increase in selectivity but a decrease in conversion that resulted in no change in yield compared to O_2 as the sole oxidizing gas.[205] An $SrO\text{-}La_2O_3/CaO$ catalyst was studied by Xu et al., who suggested the basicity of surface sites was key to increasing the selectivity of C_2 products in the presence of CO_2.[206] Shi et al. found that adding a moderate amount of CO_2 to CH_4 and O_2 (CH_4:O_2:CO_2 = 3:1:2) increased catalytic activity toward OCM. Depending on the concentration of CO_2, the reactant gases altered the

https://doi.org/10.1021/acscatal.2c01646
ACS Catal. 2022, 12, 7486−7510

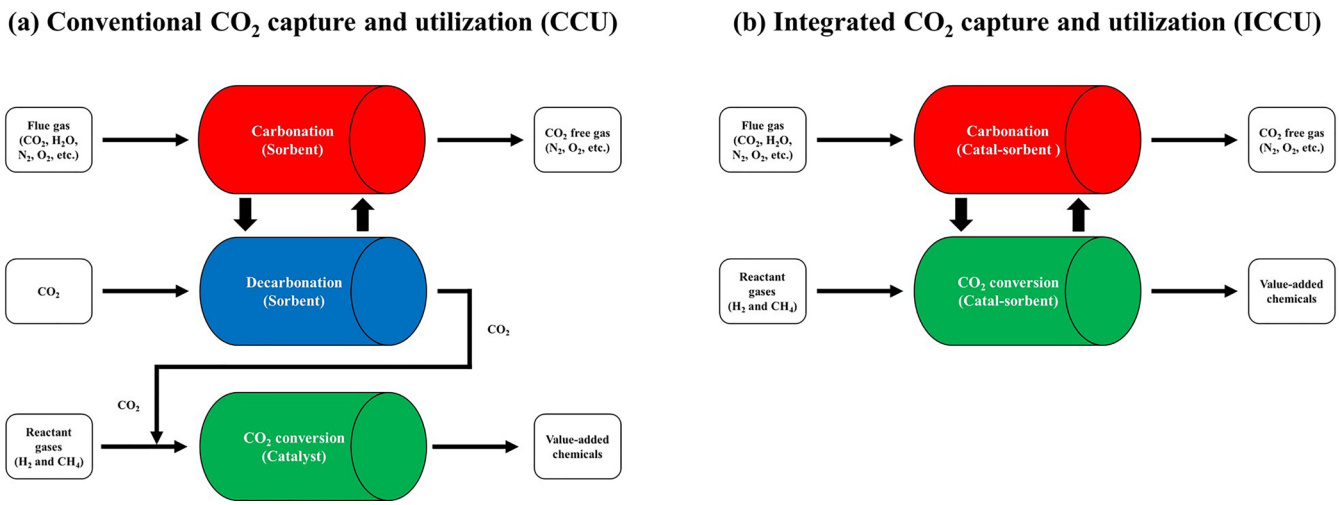

Figure 10. Schematic of the CO_2 capture and utilization (a) simple depiction of conventional CO_2 utilization where CO_2 is captured, stored, transported and then converted to valuable products (b) shows an alternative Integrated CO_2 capture and utilization (ICCU) where the catalyst-sorbent acts to selectively capture CO_2 and convert subsequently to hydrocarbons.

composition of the $Na_2WO_4/Mn/SiO_2$ catalyst.[207] The gas ratio of 3:1:2 had the highest ratio of Na_2WO_4 to $MnWO_4$ as seen under X-ray diffraction (XRD), and a strong band of WO_4 and a weak band of WO_6 were seen in their Raman spectra. The surface concentration of MO_x species was also the highest seen in X-ray photoelectron spectroscopy (XPS), and correspondingly the CH_4 conversion was the highest at 33.1% compared to other concentrations of CO_2. They surmised that the relatively high concentration of WO_4 was beneficial to the high conversion of CH_4 and selectivity to C_2H_4 and the moderate concentration of CO_2 provided favorable conditions for WO_4 formation.

Other strategies involve using CO_2 as the only oxidant source for OCM (CO_2-OCM), which is theorized to decrease the oxidative side products. The use of alternative oxidants such as CO_2 reduces the production of the oxidative side products to form C_{2+} products.[202] Nishiyama and Aika studied the effect of using CO_2 as an oxidant for OCM over the PbO−MgO catalyst.[208] Introducing CO_2 in an equal quantity as CH_4 increased the yield of C_2 products compared to the CH_4−O_2 mixture (CH_4:O_2 = 100:1). They also observed that CO yield increased monotonically with temperature, as CO_2 and CO adsorbed on the catalyst's surface and desorbed at high temperatures. They determined through isotope experiments that the CO was formed through the reverse gas shift of CO_2 and not from CH_4. Thus, the catalyst obtained a higher yield of C_2 hydrocarbons through an increase in selectivity of CH_4 oxidation to C_2. Suzuki et al. similarly studied Mg−O, Sm−O, Ca−O, Sr−O, and Sm−Mg−O catalysts for OCM prepared by decomposition of oxalates.[209] On the introduction of CO_2, C_2 yield increased with the Mg−O and Sm−Mg−O-based catalysts. With Ca−O, an increase in selectivity and activity was seen only with a low partial pressure of CO_2, and with Sr−O, the activity was curbed entirely. Chen et al. observed ∼90% selectivity toward C_2 with a reaction mixture of CH_4 and CO_2 with a La_2O_3−ZnO catalyst. The catalyst was stable in the reaction environment, with the oxide states remaining unchanged throughout testing. As seen elsewhere, the mechanism included oxidation of CH_4 by surface O species which are replenished by CO_2.[210] Korf et al. found that the Li/MgO catalyst deactivated under OCM reaction conditions could be regenerated by passing CO_2 through the catalyst. The introduction of CO_2 during OCM also precluded the deactivation of the catalyst.[211] Smith and Galuszka studied the kinetics of OCM with both O_2 and CO_2 over a Li−Pb−Ca catalyst. The formation of Li_2CO_3, which is an inactive species, reduced the conversion of methane, but there was an increase in the selectivity of C_2 formation.[212]

In summary, the use of CO_2 as the oxidizing gas for OCM, either substituting or supplementing oxygen, has seen several instances of either improving selectivity or having no effect at all. The presence of carbon dioxide increases surface O_{ads} species and reduces exothermicity of reaction, either of which could be a factor affecting the selectivity[204]

4. INTEGRATED CO_2 CAPTURE AND UTILIZATION

When sorbent-enhanced catalysts are used, the CO_2 is first captured by the sorbent support, and the captured CO_2 is converted over the embedded heterogeneous catalysts with reductant gas such as hydrogen or methane to value-added chemicals or fuels in the same reactor. Compared to the conventional CCU process (CO_2 capture, decarbonation, transport, and utilization), the ICCU process that uses SECs (CO_2 capture and direct utilization of CO_2) simplified the process and reduced the total energy required to produce value-added chemicals and fuels from CO_2 (Figure 10).

The CO_2 utilization schemes summarized in section 3 to produce hydrocarbons remain challenging to incorporate in an ICCU scheme that utilizes captured carbon. One of the prime issues is that the reaction conditions (temperature, pressure) for capture, regeneration, and utilization are sometimes different. Another area of concern is that CO_2 capture from nonideal sources can introduce contaminants that are deleterious to the stability of the catalyst and sorbent. This is further complicated by the diminishing capture and utilization efficiency of the catalyst and sorbent material over several cycles. To overcome the mismatch of reaction conditions and capture, studies usually optimally pair the capture sorbent with catalytic reaction conditions in which the CO_2 desorption and subsequent conversion to the value-added chemical have similar reaction conditions. Additionally, researchers have started to improve catalyst and sorbent stability with the addition of metal promoters to staunch the sintering of the materials over several cycles. Nevertheless, the ICCU process has attracted great

https://doi.org/10.1021/acscatal.2c01646
ACS Catal. 2022, 12, 7486−7510

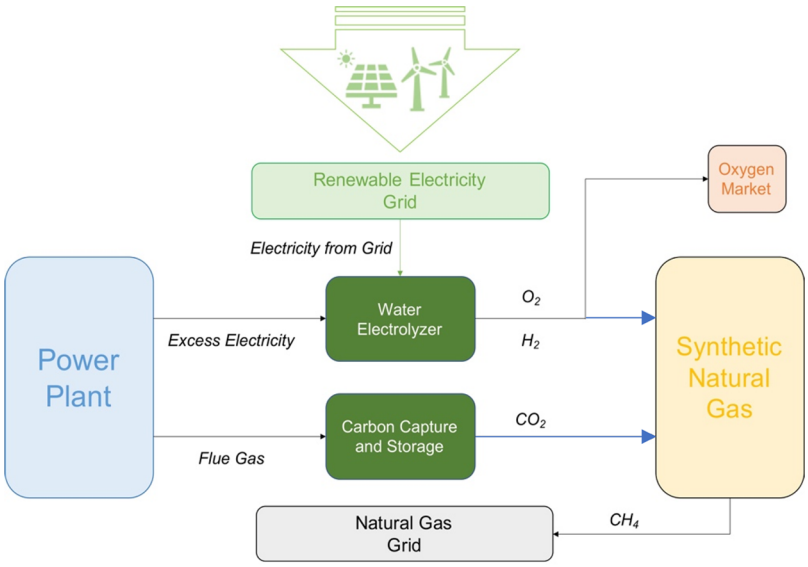

Figure 11. Schematic of renewable natural gas derived from captured CO_2 and hydrogen generated from electrolysis using excess electricity from the renewable and power plant grid.

attention in reducing total thermal energy and ensuring a simplified capture and conversion process.

4.1. Methanation. Among the ICCU reaction pathways that use SECs, the methanation ($CO_2 + 4H_2 \rightarrow CH_4 + H_2O$) reaction is the most straightforward and suitable strategy for large-scale CO_2 reduction.[213] Natural gas, which consists of mainly methane, emits the smallest amount of CO_2 per energy unit compared to other fossil fuels and can be used as an important energy carrier in addition to electricity.[214] Large-scale integration of renewable energy such as wind and solar energy into the existing electricity framework is challenging because of unstable power supply and an imbalance between the power grid in matching the power supply and demand.[215] The power-to-gas (P2G) technology has been considered to mitigate fluctuating and intermittent renewable energy sources in integrated energy storage systems.[214−217] The P2G process consists of H_2 production by water electrolysis using surplus energy in a power plant or renewable energy sources and methane production using the methanation process from captured CO_2 and renewable H_2, which is connected to the natural gas grid (Figure 11).

In practice, the thermodynamics and reaction rate are the most concerning factors, although the CO_2 methanation takes place at atmospheric pressure and low temperature.[218] The novel metal catalysts such as Ru, Rh, and Pt have excellent catalytic activity at lower temperatures compared to transition metal-based catalysts such as Co, Fe, and Ni.[219] The Ni-based catalyst has been widely investigated because of its relatively low price, in spite of low-temperature catalytic activities.[220,221] CO_2 methanation, which is an exothermic reaction, is favored at lower temperatures; the reverse reaction takes place at temperatures higher than 627 °C.[222−224] At low temperatures, the reaction rate is slow although high CO_2 conversion and CH_4 selectivity are achieved.[218] On the other hand, a high operating temperature will reduce the CO_2 conversion according to the thermodynamic equilibrium. Moreover, the RWGS reaction and dry methane reforming (DMR) also occur, leading to low selectivity for methane.[218] Therefore, it is important to introduce proper catalysts and optimize the operating parameters for high CO_2 conversion, CH_4 selectivity, and fast reaction rate for methanation in the ICCU process.

Zheng et al. developed sorption-enhanced catalysts, 5% Ru,10%CaO/γ-Al_2O_3 for the CO_2 capture and direct methanation at 320 °C and proposed a mechanism for surface reactions for the CO_2 chemisorption and direct methanation.[225] During the CO_2 adsorption step, CO_2 is rapidly adsorbed onto the CaO site, and metallic ruthenium undergoes partial oxidation under feed gas containing CO_2, O_2, and steam. Subsequently, under the H_2 condition, the methanation process follows elementary steps: (1) reduction of partially oxidized ruthenium, (2) spillover of adsorbed CO_2 from the CaO to the adjacent reduced Ru sites, (3) dissociative chemisorption of H_2 on Ru, (4) dissociation of CO_2 and H_2 to complexes, and (5) catalytic conversion to CH_4. Several SECs, consisting of Na_2O as an adsorbent and Ni-based bimetallic catalysts, were also developed to replace some Ru with Ni for possible additional cost reduction.[226,227] Ni-based SECs cannot convert CO_2 adsorbed to methane because of oxidation of Ni metal after CO_2 chemisorption under O_2 containing flue gas conditions. Small amounts of precious metal (<1% Pt, Pd, or Ru) enhance the reduction and activation of Ni-containing SEC for direct methanation even after O_2 exposure in the flue gas at 320 °C. However, the SECs consist of a small amount of sorbent materials, and CO_2 is chemisorbed onto sorbent sites, resulting in extremely low CO_2 capture capacity and CH_4 productivity and selectivity.

Bermejo-Lopez et al. synthesized Ni/Al_2O_3 catalysts containing CaO or Na_2CO_3 that contain basic sites with a varying affinity for the adsorption of CO_2.[228] The amount of CH_4 was always higher for the CaO containing catalysts owing to the higher total basicity. These catalysts provided different temperature ranges for CH_4 formation, between 200 and 600 °C for CaO containing samples and a narrow temperature range of 200−400 °C for Na_2CO_3 containing samples. Jo et al. synthesized Ni/CaO SEC via the sol−gel method and investigated the influence of temperature (400−700 °C) on direct methanation. CO_2 capture capacity showed a positive correlation with temperatures.[229] They found that the captured CO_2 was converted completely to CH_4 at 500, and carbonation

https://doi.org/10.1021/acscatal.2c01646
ACS Catal. 2022, 12, 7486−7510

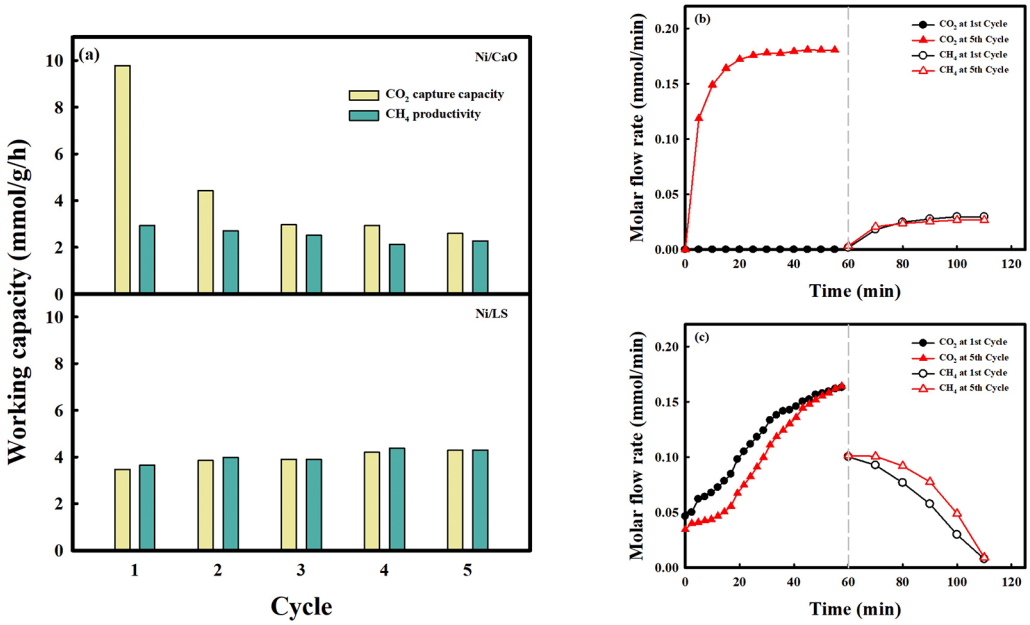

Figure 12. (a) Comparison of working CO_2 capture capacity and CH_4 productivity of Ni/CaO and Ni/LS SECs; molar flow rate of CO_2 and CH_4 of (b) Ni/CaO and (c) Ni/LS SECs at 1 and 5 cycles in a rapid cyclic system. Reproduced with permission from Reference 230. Copyright 2021, Elsevier.

of $CaCO_3$ could not occur. The Ni/CaO SECs showed excellent multicycle stability with high CO_2 capture capacity and CH_4 productivity at 500 °C.

Using the solid-state reaction, Jo et al. also prepared nickel−lithium−silicate (Ni/LS) SECs.[230] The working CO_2 capture capacity and CH_4 productivity of Ni/LS SECs were investigated and compared with Ni/CaO SECs in a rapid cyclic system. The Ni/CaO SECs exhibited approximately three times higher working CO_2 capture capacity at 550 °C for 1 h at the first rapid cycle than the Ni/LS SECs. However, the working CO_2 capture capacity of Ni/CaO decreased dramatically in the rapid cyclic system because the captured CO_2 by CaO is partially regenerated with very slow direct methanation for 1 h at 550 C. On the other hand, the Ni/LS SECs showed stable working CO_2 capture capacity and CH_4 productivity with the fast kinetics of direct methanation (Figure 12). Park et al. prepared catalytic sorbents by physically mixing $NaNO_3$/MgO and Ru/Al_2O_3 catalysts.[231] They found that the catalytic sorbent decreased CO_2 sorption capacity due to the deactivation of the $NaNO_3$/MgO sorbent. In-situ FTIR measurements were performed during the CO_2 methanation over 1% Ru/Al_2O_3 and 5% $NaNO_3$/1%Ru/Al_2O_3. They hypothesized that carbonyl species were likely reaction intermediates over 1%Ru/Al_2O_3, while formate species were spectators. On the other hand, for 5% $NaNO_3$/1%Ru/Al_2O_3, both carbonyl and formate species, along with carbonate and bicarbonate species, were likely reaction intermediates. Reaction order measurements for CO_2 and H_2 combined with hypothetical reaction mechanisms and rate laws for CO_2 methanation were developed for the two catalysts.

4.2. Reverse Water−Gas Shift. Direct RWGS reaction using SECs has also been studied because RWGS is another promising reaction in CO_2 hydrogenation, which can be connected with the FT reaction for the production of value-added chemicals such as hydrocarbon fuels, methanol, and light olefins using the produced syngas. The RWGS reaction is thermodynamically favored at high temperatures (endothermic reaction) and a high H_2/CO_2 ratio.[232] The CO can be a major product at temperatures above 700 °C because CO methanation is the main reaction below 700 °C. Therefore, the sintering of catalysts and sorbent materials is the most important concern of the RWGS reaction for ICCU. Until now, the studies for the H_2/CO ratio in the outlet gas via RWGS in the ICCU process are limited. Therefore, extensive studies on the H_2/CO ratio are needed under different operating conditions (space velocity, H_2 concentration in feed, catalyst/sorbent ratio, etc.) to meet the stoichiometric ratio required for FT reaction or methanol production. Bobadilla et al. prepared a catalyst comprising earth-abundant chemical elements (FeCrCu/K/MgO−Al_2O_3).[233] The catalyst exhibited high stability and high carbon balance but an H_2/COx ratio (ca. 40 times) higher than the stoichiometric ratio of methanol synthesis or FT synthesis at 550 °C. Sun et al. integrated the CO_2 capture and the RWGS reaction.[234] They found that the MFM (Ca1Ni0.1Ce0.033) exhibited outstanding CO yield (7.3 mmol g^{-1}) over 20 cycles at the same temperature of 650 °C, but the unreacted CO_2 was released, leading to relatively low CO_2 conversion (51.8%). Jo et al. investigated the temperature-programmed surface reaction (TPSR) using Ni/CaO SECs at different H_2 concentrations (10 and 100%) from 100 to 800 °C after CO_2 sorption for both methanation and direct RWGS reaction in the ICCU process.[235] The direct methanation and RWGS depended on the reaction temperature and H_2 concentration (e.g., $H_2/CaCO_3$ ratio). In the direct RWGS, decarbonation and subsequent reaction with diluted H_2 concentration (10 vol %) formed a high yield of CO at 700 °C, but the cyclic stability was not investigated.

4.3. Dry Methane Reforming. In addition to direct hydrogenation of CO_2, such as methanation and RWGS, other CO_2 utilization technologies were studied for the ICCU process that uses SECs. Several researchers have combined CaL CO_2 capture with DRM (CaLDRM), which converts two greenhouse gases (CO_2 and CH_4) into industrial feedstock syngas.[235−237] Because H_2 is industrially produced from methane, DRM is considered more economical and efficient than CO_2 hydrogenation technologies. Moreover, a higher thermodynamic equilibrium was observed in the conversion of $CaCO_3$ by CH_4, compared to the conversion with H_2 at a high temperature

https://doi.org/10.1021/acscatal.2c01646
ACS Catal. 2022, 12, 7486−7510

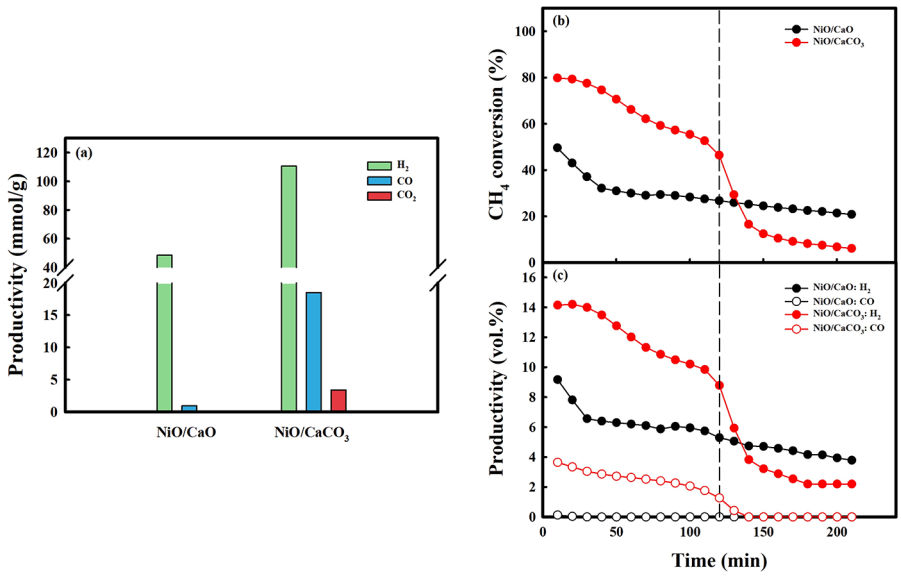

Figure 13. Syngas production performances in the CH_4 conversion step: (a) syngas (H_2 and CO) productivity and capacity for desorbing CO_2, (b) CH_4 conversion, and (c) syngas mole fraction obtained by utilizing NiO/CaO and NiO/$CaCO_3$ under the 10 vol % CH_4 condition at 650 °C. Reproduced with permission from Reference 239. Copyright 2022, Royal Society of Chemistry.

(>600 °C).[235] Kim et al. demonstrated the feasibility of coupled CO_2 capture and conversion reactions performed at 720 °C using a mixture of CaO (CO_2 sorbent) and Ni/MgO−Al_2O_3 (DRM catalyst).[238] The released CO_2 (regeneration of the CO_2 sorbent) is converted into syngas with an approximately equimolar ratio of H_2 to CO with minimal CO_2 slip; however, the CO_2 uptake decreases during 10 cycles from thermal sintering of CaO at 720 °C. Tian et al. coupled the CaL-based CO_2 capture and DRM in ICCU, employing a CaO/Ni bifunctional sorbent catalyst to exploit the possibility of producing syngas from waste CO_2 in an energy-efficient manner.[237] Compared with conventional CaL processes, the captured CO_2 was desorbed with superior reaction kinetics. The desorbed CO_2 reacted with CH_4 at 800 °C when Ni-catalyzed CH_4 reforming was integrated with $CaCO_3$ regeneration, following Le Chatelier's principle. However, the high operating temperature for high DRM performance caused a decrease in the CO_2 capture capacity with the cycle number because of the thermal sintering of the CaO/$CaCO_3$ phase. This low amount of CO_2 in the following DRM step marginally decreased the syngas yield and coke formation. Although the deposited carbon could be gasified via the reverse Boudouard reaction in the following CO_2 capture step, the deposited carbon is accumulated in the DRM process. Several researchers have been focused on improving the multicycle stability of Ni-CaO based materials for CaLDRM in the ICCU.

Hu et al. synthesized modified Ni−Ca materials with structural stabilizers to serve as the bifunctional material for CaL combined with the DRM process.[236] For Ni and CeO_2 nanoparticles coloaded on ZrO_2-coated $CaCO_3$ (NiCe/Ca@Zr), the ZrO_2 layer stabilized the $CaCO_3$ support and served as a barrier to prevent the loaded Ni from agglomeration during the cyclic tests. For Ni-supported CaO_2-modified CaO materials (Ni/CaCe), the CeO_2 acted as a structure that stabilized enhanced the CO_2 affinity of CaO and the low-temperature activity of Ni, leading to higher CO_2 capture and catalytic conversion of CO_2 at 650 °C. Moreover, the CeO_2 as a structure stabilizer improved the sinter resistance of CaO and the Ni dispersion, maintaining CaL kinetics and DRM activity. Jo et al. proposed a new type of highly efficient strategy for producing CO and syngas in a cyclic ICCU process employing a coke-promoted Ni/CaO (C−Ni/CaO) SECs prepared by CH_4 pretreatment, in which NiO was reduced to Ni and coke was deposited on the surface of Ni sites (Figure 13).[239] Previous studies on the DRM process mainly focused on the high resistance to thermal sintering and alleviation of coke formation by conducting DRM at high temperatures (>800 °C). However, they alleviated the thermal sintering by conducting DRM in the ICCU at a relatively low temperature (650 °C) and then applied the coke as a source of CO production. In the CO_2 conversion step, the coke was gasified by CO_2 via the reverse Boudouard reaction. The residual CO_2 was simultaneously stored in the $CaCO_3$ phase, thus enabling the high consumption of CO_2 and CO production. In the subsequent CH_4 conversion step, $CaCO_3$ was regenerated, and the desorbed CO_2 was converted with CH_4 to syngas via DRM. Simultaneously, hydrogen was produced, and the carbon source to produce CO in the CO_2 conversion step was supplied by the CH_4 decomposition. The C−Ni/CaO SECs exhibited stable performances during 10th in the cyclic CO_2 and CH_4 conversion.

5. CONCLUSIONS AND FINAL PERSPECTIVE

This perspective discussed CO_2 capture and conversion schemes that incorporate sorption-enhanced catalysts. Although there has been progress in using SECs for ICCU, various issues must be addressed, including the limited CO_2 capture and regeneration efficiency, thermostability, product stream, and economic feasibility. There are four areas of primary consideration in advancing SECS:

(1) Improving the thermostability of the oxide sorbent-support for long-term stability and enhanced sorption and desorption rates. Ideally, sorbent-enhanced catalysts should have a high CO_2 capture capacity and a rapid sorption rate. However, the flux of CO_2 and the carbonation−calcination cycles can introduce thermal stress to SECs that can drastically decline the performance of the solid sorbents and catalyst nanoparticles. To

https://doi.org/10.1021/acscatal.2c01646
ACS Catal. 2022, 12, 7486−7510

improve the evaluation of structure−function properties, future research strategies should incorporate fundamental studies of the SECs at elevated temperatures to ascertain the mechanistic groundwork of the deactivation mechanism that limits performance. The structural changes of materials and reaction mechanisms during the cyclic ICCU process are most likely distinct from that of conventional CO_2 capture and utilization processes. *In situ* and *in operando* strategies that can analyze the surface and bulk characteristics, such as surface-enhanced-Raman spectroscopy, XRD, and X-ray absorption spectroscopy, will be helpful for studying the deactivation mechanisms for SECs according to the types of materials (sorbents and catalysts) used and reaction conditions such as feed gas composition and temperature. For example, reoxidation of embedded catalysts in SECs by oxygen in flue gas during the CO_2 capture step can promote the gasification of coke deposited on the surface during DRM but may have a negative influence on the subsequent catalytic conversion and CO_2 capture performances.

For sorbent materials selection, CaO is the most used oxide sorbent but suffers from drastic performance loss due to repeated carbonation−calcination cycles. The sintering of the sorbent support will decrease CO_2 capture performance and, as discussed, has been widely reported because of severe conditions for decarbonation or direct utilization. To improve stability, a variety of inert stabilizers, such as ZrO_2 and Al_2O_3, have been incorporated into the intraparticle region of sorbent materials to enhance their textural properties and thermal stability. Generally, the inert materials are in the form of a second phase to slow down the aggregation or sintering of the alkali or alkali earth metal sorbents. The properties of the stabilizers can range, but generally, the materials have a higher Tammann temperature than the sorbent. Thus, the goal of the stabilizer is to improve the surface area and increase the melting point of the newly formed composite materials. For example, Al-doped CaO sorbents have improved durability over the multiple carbonation/decarbonation cycles compared to CaO only. The improved stability is due to the formation of inert composite materials ($Ca_{12}Al_{14}O_{33}$) that provide a stable framework to inhibit the severe sintering of CaO particles. The addition of an excessive amount of stabilizers can considerably improve the cyclic stability of the composite materials but can lower the maximum theoretical CO_2 capture capacity. Therefore, there is a need for a more judicious selection of stabilizers that can maximize the cyclability and CO_2 capture capacity.

Low temperature (LT) CO_2 sorbents (e.g., zeolites, MOFs, K_2CO_3, or Na_2CO_3) have good CO_2 capture and regenerability at temperatures below 100 °C. Their properties are ideal for some CO_2 capture and conversion schemes requiring a low regeneration temperature, such as methanol production. Nevertheless, LT sorbents have unique challenges in comparison to their high-temperature counterparts (CaO), where the sorbents can decompose at temperatures lower than their Tammann temperatures. The deterioration of the sorbents and kinetics for CO_2 adsorption/desorption can be exacerbated in the presence of water and have sensitivity to temperature fluxes. Promoters and stabilizers such as activated carbon, Al_2O_3, SiO_2, and TiO_2 have been introduced widely to LT CO_2 sorbents to improve the durability and diffusion-limited gas exchange that sometimes prevents adsorption of CO_2 at low temperatures. Similar to their HT counterparts, incorporating promoters or stabilizers can decrease the CO_2 capture capacity. The lower energy penalty for CO_2 capture and utilization is appealing. Future endeavors should focus on the rational addition of promoters and stabilizers and their influence on the SECs' cyclic stability and subsequent reaction pathways.

(2) ICCU valorization strategies that incorporat SECS should include more strategies to produce high-value hydrocarbons with C_2^+ products such as olefins, higher alcohols, and liquid fuels. Ideally, these CO_2-derived products would replace petrochemical-derived feedstocks for plastics, fine chemicals, and fuels. The ICCU schemes for the capture of CO_2 and subsequent conversion to methane and syngas are quite mature. This is mainly due to the high barrier for carbon−carbon coupling and, in some cases, enhanced selectivity to the C_1 products. As discussed in this perspective, researchers circumvent this limitation in traditional CO_2 utilization schemes by focusing on methanol or syngas-mediated routes to C_2^+ products. However, the use of such strategies for ICCU is relatively nascent and needs additional research for feasibility. This must involve efforts to elucidate the reaction mechanism and selectivity for catalysts developed and control the reaction conditions to produce target products. Optimization of the operating conditions such as high-temperature environments and feed gas composition should also be considered.

Compared with conventional catalytic reactions, there are many pathways for SEC deactivation including reoxidation, sintering, poisoning, and carbon deposition, due to the thermal fluxes involved in the cyclic CO_2 capture and utilization. The addition of promoters is useful for improving catalytic performance and prolonging the lifetime of SECS. A strategy to decrease the occurrence of partial oxidation is the addition of noble metal promoters, such as Ru, Rh, Pt, and Pd, that can enhance the reducibility of catalysts. Furthermore, coupling the alkali oxide sorbents with a support that has inherent strong metal−support interaction with the catalyst, such as spinels ($NiAl_2O_4$) or perovskite oxides ($LaNiO_3$ and $LaFeO_3$), could be helpful to reduce the sintering of the embedded catalysts during the thermal cycles. To reduce coke formation, it is advantageous to add materials with high oxygen mobility, such as CeO_2 or Fe_2O_3, because the lattice oxygen interacts with adsorbed carbon to promote gasification of the formed coke. However, further research needs to be done to ascertain how these additional promoters improve the catalyst performance and influence the CO_2 sorption and desorption capabilities of the support.

(3) Improving the cost of the SEC strategies to higher value products by reducing the costs for renewable hydrogen. CO_2 reduction experiments either use hydrogen or methane to upgrade the products. The use of renewable hydrogen is derived from the electrolysis of water, and its generation is connected to the price of electricity. Currently, the production costs for CO_2-based chemicals and fuels are several times higher than those for conventional counterparts made from petrochemicals.

https://doi.org/10.1021/acscatal.2c01646
ACS Catal. 2022, 12, 7486−7510

Thus, competitively it is ideal for decreasing the costs for synthesized chemicals from CO_2 in which ICCU is useful.

A significant component of the costs for CO_2 utilization is the costs associated with hydrogen production. The costs can be contingent on the targeted CO_2-derived products. In the case of producing renewable hydrogen using electrolysis (green hydrogen), the process relies on the capital cost of the electrolyzer and the average cost of purchased electricity. Thus, hydrogen production costs are susceptible to electricity prices. For utilization of around 40−50% and an average electricity prices of 42−52 $/MWh, electricity would make up more than half of the hydrogen production costs.[240] This signifies that the overall cost of CO_2 utilization will be greatly affected by the energy requirements to produce hydrogen. Alternatively, steam methane reforming (SMR) still accounts for almost the entirety of the global demand for hydrogen: 97% (gray hydrogen). This process generates a large amount of CO_2 emissions (9 kg of CO_2 per 1 kg of H_2 produced), accounting for roughly 830 Mt_{CO2}/yr in 2018.[241] Integrating CCS into the SMR may allow for the production of low emission hydrogen (blue hydrogen). Hydrogen production cost from SMR coupled with CCS is mainly dominated by natural gas prices. Furthermore, SMR is capital intensive, requires high incurring operating costs, and largely depends on the site-specific nature of carbon storage reservoirs.[241] Incorporating CCU strategies could generate additional revenue to help offset the cost of storage. Further study into the economics of combining carbon capture utilization and storage (CCUS) with SMR is needed to reduce hydrogen production costs and improve the commercial viability of the process. Efforts to decrease the cost of hydrogen should also be beneficial for the expenses of CO_2-derived products, making it possible to produce at either comparable or lower costs to the current market value.

(4) Developing strategies in which catalyst and sorbent can effectively function in "real" streams of CO_2 that contain variable concentrations of CO_2 along with relative humidity (H_2O) and acid gases (H_2S, SO_2, and HCl). Most research in ICCU and CO_2 utilization use ideal streams of CO_2 with minimal contaminants. However, research into the efficacy of sorbent-enhanced catalysts and the additional inherent challenges of using more realistic streams are still in their nascency and must be explored further. While CO_2 can be sourced directly from the air, the materials discussed in this perspective are utilized primarily in pre- and postcombustion atmospheres. The flue gas streams are notoriously complex. The most common impurities include N_2, O_2, and H_2O from air combustion products, acidic gases such as H_2S, SOx, NOx, HCl, hydrocarbons, and trace metals including Hg, Se, and As. The presence of H_2O can significantly influence the capture efficiency of the solid sorbents where H_2O can compete with the same active sites as CO_2. The presence of H_2O can also accelerate the sintering of the embedded catalyst nanoparticles at elevated temperatures. Furthermore, the presence of sulfur compounds can substantially diminish the performance of the catalyst and sorbent over time. Thus, real gases will increase the capital costs not considered with the current research thrusts.

Despite research challenges, policy support by government and industry stakeholders is a significant component of the adoption of alternative technologies for value-added chemical production. The development of SECs can potentially decrease the separation and transportation costs of CO_2-derived products. But the CO_2-derived products would only be competitive against conventional processes once policies incentivize such progress. Early adoption of policies would help spur new markets for CO_2-derived products. The policy decisions must be informed by life cycle analysis combined with experimental and theoretical research. Life cycle analysis is necessary for the marketability of ICCU in CO_2 mitigation schemes. The climate benefits of ICCU are not exactly clear, and the potential climate benefits for different reaction pathways are unknown. Growth in this field must couple experts from computational science, experimental heterogeneous catalysis and computational researchers, materials science and engineering, and life-cycle analysis to promote its development.

■ AUTHOR INFORMATION

Corresponding Author

Kandis Leslie Gilliard-AbdulAziz − *Department of Chemical and Environmental Engineering, University of California−Riverside, Riverside, California 92521, United States; Department of Material Science and Engineering, University of California−Riverside, Riverside, California 92521, United States;* orcid.org/0000-0002-1706-9552; Email: klabdulaziz@engr.ucr.edu

Authors

Seongbin Jo − *Department of Chemical and Environmental Engineering, University of California−Riverside, Riverside, California 92521, United States;* orcid.org/0000-0002-6622-3616

Luz Cruz − *Department of Material Science and Engineering, University of California−Riverside, Riverside, California 92521, United States*

Soham Shah − *Department of Chemical and Environmental Engineering, University of California−Riverside, Riverside, California 92521, United States;* orcid.org/0000-0003-0277-3835

Somchate Wasantwisut − *Department of Chemical and Environmental Engineering, University of California−Riverside, Riverside, California 92521, United States*

Annette Phan − *Department of Chemical and Environmental Engineering, University of California−Riverside, Riverside, California 92521, United States;* orcid.org/0000-0002-3024-4343

Complete contact information is available at: https://pubs.acs.org/10.1021/acscatal.2c01646

Notes

The authors declare no competing financial interest.

■ ACKNOWLEDGMENTS

This work was partially supported by the National Science Foundation (CBET: No. 2143578). We are grateful for the financial support.

REFERENCES

(1) Reay, D. S.; Smith, P.; Christensen, T. R.; James, R. H.; Clark, H. Methane and Global Environmental Change. *Annu. Rev. Env Resour* **2018**, *43*, 165−192.

(2) Turner, A. J.; Frankenberg, C.; Kort, E. A. Interpreting contemporary trends in atmospheric methane. *P Natl. Acad. Sci. USA* **2019**, *116* (8), 2805−2813.

(3) Yusuf, R. O.; Noor, Z. Z.; Abba, A. H.; Hassan, M. A. A.; Din, M. F. M. Methane emission by sectors: A comprehensive review of emission sources and mitigation methods. *Renew Sust Energ Rev.* **2012**, *16* (7), 5059−5070.

(4) Anderson, K.; Peters, G. The trouble with negative emissions. *Science* **2016**, *354* (6309), 182−183.

(5) Peters, G. P.; Andrew, R. M.; Canadell, J. G.; Friedlingstein, P.; Jackson, R. B.; Korsbakken, J. I.; Le Quere, C.; Peregon, A. Carbon dioxide emissions continue to grow amidst slowly emerging climate policies. *Nat. Clim Change* **2020**, *10* (1), 3−6.

(6) Scott, K.; Smith, C. J.; Lowe, J. A.; Garcia-Carreras, L. Demand vs supply-side approaches to mitigation: What final energy demand assumptions are made to meet 1.5 and 2 degrees C targets? *Global Environ. Chang* **2022**, *72*, 102448.

(7) Zeebe, R. E. History of Seawater Carbonate Chemistry, Atmospheric CO2, and Ocean Acidification. *Annu. Rev. Earth Pl Sc* **2012**, *40*, 141−165.

(8) Urbarova, I.; Foret, S.; Dahl, M.; Emblem, A.; Milazzo, M.; Hall-Spencer, J. M.; Johansen, S. D. Ocean acidification at a coastal CO_2 vent induces expression of stress-related transcripts and transposable elements in the sea anemone Anemonia viridis. *PLoS One* **2019**, *14* (5), No. e0210358.

(9) Wepener, V. Statement from world aquatic scientific societies on the need to take urgent action against human-caused climate change, based on scientific evidence. *Afr J. Aquat Sci.* **2020**, *45* (4), 383−385.

(10) Yu, Z.; McAndrews, J. H.; Eicher, U. Middle Holocene dry climate caused by change in atmospheric circulation patterns: Evidence from lake levels and stable isotopes (vol 25, pg 251, 1997). *Geology* **1997**, *25* (5), 251.

(11) Stevenson, R. L. Climate Change: Evidence and Causes: Update 2020. *Integr Environ. Asses* **2020**, *16* (5), 793−794.

(12) Bui, M.; Adjiman, C. S.; Bardow, A.; Anthony, E. J.; Boston, A.; Brown, S.; Fennell, P. S.; Fuss, S.; Galindo, A.; Hackett, L. A.; Hallett, J. P.; Herzog, H. J.; Jackson, G.; Kemper, J.; Krevor, S.; Maitland, G. C.; Matuszewski, M.; Metcalfe, I. S.; Petit, C.; Puxty, G.; Reimer, J.; Reiner, D. M.; Rubin, E. S.; Scott, S. A.; Shah, N.; Smit, B.; Trusler, J. P. M.; Webley, P.; Wilcox, J.; Mac Dowell, N. Carbon capture and storage (CCS): the way forward. *Energ Environ. Sci.* **2018**, *11* (5), 1062−1176.

(13) Katelhon, A.; Meys, R.; Deutz, S.; Suh, S.; Bardow, A. Climate change mitigation potential of carbon capture and utilization in the chemical industry. *P Natl. Acad. Sci. USA* **2019**, *116* (23), 11187−11194.

(14) Honda, S.; Mori, T.; Goto, H.; Sugimoto, H. Carbon-dioxide-derived unsaturated alicyclic polycarbonate: Synthesis, characterization, and post-polymerization modification. *Polymer* **2014**, *55* (19), 4832−4836.

(15) Cao, H.; Zhang, R. Y.; Zhou, Z. Z.; Liu, S. J.; Tao, Y. H.; Wang, F. S.; Wang, X. H. On-Demand Transformation of Carbon Dioxide into Polymers Enabled by a Comb-Shaped Metallic Oligomer Catalyst. *ACS Catal.* **2022**, *12* (1), 481−490.

(16) Burkart, M. D.; Hazari, N.; Tway, C. L.; Zeitler, E. L. Opportunities and Challenges for Catalysis in Carbon Dioxide Utilization. *ACS Catal.* **2019**, *9* (9), 7937−7956.

(17) Thorat, S. D.; Phillips, P. J.; Semenov, V.; Gakh, A. Physical properties of aliphatic polycarbonates made from CO_2 and epoxides. *J. Appl. Polym. Sci.* **2003**, *89* (5), 1163−1176.

(18) Williams, C. K.; Hillmyer, M. A. Polymers from renewable resources: A perspective for a special issue of polymer reviews. *Polym. Rev.* **2008**, *48* (1), 1−10.

(19) Panzone, C.; Philippe, R.; Nikitine, C.; Vanoye, L.; Bengaouer, A.; Chappaz, A.; Fongarland, P. Catalytic and Kinetic Study of the CO_2 Hydrogenation Reaction over a Fe-K/Al_2O_3 Catalyst toward Liquid and Gaseous Hydrocarbon Production. *Ind. Eng. Chem. Res.* **2021**, *60* (46), 16635−16652.

(20) Ye, R. P.; Ding, J.; Gong, W. B.; Argyle, M. D.; Zhong, Q.; Wang, Y. J.; Russell, C. K.; Xu, Z. H.; Russell, A. G.; Li, Q. H.; Fan, M. H.; Yao, Y. G. CO_2 hydrogenation to high-value products via heterogeneous catalysis. *Nat. Commun.* **2019**, *10*, 5698.

(21) Sahoo, P. K.; Zhang, Y.; Das, S. CO_2-Promoted Reactions: An Emerging Concept for the Synthesis of Fine Chemicals and Pharmaceuticals. *ACS Catal.* **2021**, *11* (6), 3414−3442.

(22) Ramirez, A.; Dutta Chowdhury, A.; Dokania, A.; Cnudde, P.; Caglayan, M.; Yarulina, I.; Abou-Hamad, E.; Gevers, L.; Ould-Chikh, S.; De Wispelaere, K.; van Speybroeck, V.; Gascon, J. Effect of Zeolite Topology and Reactor Configuration on the Direct Conversion of CO_2 to Light Olefins and Aromatics. *ACS Catal.* **2019**, *9* (7), 6320−6334.

(23) Tu, C. Y.; Nie, X. W.; Chen, J. G. G. Insight into Acetic Acid Synthesis from the Reaction of CH_4 and CO_2. *ACS Catal.* **2021**, *11* (6), 3384−3401.

(24) Zhou, C.; Asundi, A. S.; Goodman, E. D.; Hong, J.; Werghi, B.; Hoffman, A. S.; Nathan, S. S.; Bent, S. F.; Bare, S. R.; Cargnello, M. Steering CO_2 hydrogenation toward C-C coupling to hydrocarbons using porous organic polymer/metal interfaces. *Proc. Natl. Acad. Sci. U. S. A.* **2022**, *119* (7), No. e2114768119.

(25) De Ras, K.; Van de Vijver, R.; Galvita, V. V.; Marin, G. B.; Van Geem, K. M. Carbon capture and utilization in the steel industry: challenges and opportunities for chemical engineering. *Curr. Opin Chem. Eng.* **2019**, *26*, 81−87.

(26) Gur, T. M. Carbon Dioxide Emissions, Capture, Storage and Utilization: Review of Materials, Processes and Technologies. *Prog. Energy Combust. Sci.* **2022**, *89*, 100965.

(27) De, S.; Dokania, A.; Ramirez, A.; Gascon, J. Advances in the Design of Heterogeneous Catalysts and Thermocatalytic Processes for CO_2 Utilization. *ACS Catal.* **2020**, *10* (23), 14147−14185.

(28) Morales-Salvador, R.; Gouveia, J. D.; Morales-Garcia, A.; Vines, F.; Gomes, J. R. B.; Illas, F. Carbon Capture and Usage by MXenes. *ACS Catal.* **2021**, *11* (17), 11248−11255.

(29) Guo, S. Y.; Asset, T.; Atanassov, P. Catalytic Hybrid Electrocatalytic/Biocatalytic Cascades for Carbon Dioxide Reduction and Valorization. *ACS Catal.* **2021**, *11* (9), 5172−5188.

(30) Renfrew, S. E.; Starr, D. E.; Strasser, P. Electrochemical Approaches toward CO_2 Capture and Concentration. *ACS Catal.* **2020**, *10* (21), 13058−13074.

(31) Al-Attas, T. A.; Marei, N. N.; Yong, X.; Yasri, N. G.; Thangadurai, V.; Shimizu, G.; Siahrostami, S.; Kibria, M. G. Ligand-Engineered Metal-Organic Frameworks for Electrochemical Reduction of Carbon Dioxide to Carbon Monoxide. *ACS Catal.* **2021**, *11* (12), 7350−7357.

(32) Ra, E. C.; Kim, K. Y.; Kim, E. H.; Lee, H.; An, K.; Lee, J. S. Recycling Carbon Dioxide through Catalytic Hydrogenation: Recent Key Developments and Perspectives. *ACS Catal.* **2020**, *10* (19), 11318−11345.

(33) Bai, S. T.; Zhou, C.; Wu, X.; Sun, R. Y.; Sels, B. Suppressing Dormant Ru States in the Presence of Conventional Metal Oxides Promotes the Ru-MACHO-BH-Catalyzed Integration of CO2 Capture and Hydrogenation to Methanol. *ACS Catal.* **2021**, *11* (20), 12682−12691.

(34) Park, S. J.; Bukhovko, M. P.; Jones, C. W. Integrated capture and conversion of CO2 into methane using $NaNO_3$/MgO + Ru/Al_2O_3 as a catalytic sorbent. *Chem. Eng. J.* **2021**, *420*, 130369.

(35) Sun, S. Z.; Sun, H. M.; Williams, P. T.; Wu, C. F. Recent advances in integrated CO_2 capture and utilization: a review. *Sustain Energ Fuels* **2021**, *5* (18), 4546−4559.

(36) Lawson, S.; Baamran, K.; Newport, K.; Rezaei, F.; Rownaghi, A. Screening of Adsorbent/Catalyst Composite Monoliths for Carbon Capture-Utilization and Ethylene Production. *Acs Appl. Mater. Inter* **2021**, *13* (46), 55198−55207.

(37) Dunstan, M. T.; Donat, F.; Bork, A. H.; Grey, C. P.; Muller, C. R. CO_2 Capture at Medium to High Temperature Using Solid Oxide-Based Sorbents: Fundamental Aspects, Mechanistic Insights, and Recent Advances. *Chem. Rev.* **2021**, *121* (20), 12681−12745.

https://doi.org/10.1021/acscatal.2c01646
ACS Catal. 2022, 12, 7486−7510

(38) Samanta, A.; Zhao, A.; Shimizu, G. K. H.; Sarkar, P.; Gupta, R. Post-Combustion CO_2 Capture Using Solid Sorbents: A Review. *Ind. Eng. Chem. Res.* **2012**, *51* (4), 1438−1463.
(39) Chang, R. B.; Wu, X. Y.; Cheung, O.; Liu, W. Synthetic solid oxide sorbents for CO_2 capture: state-of-the art and future perspectives. *J. Mater. Chem. A* **2022**, *10* (4), 1682−1705.
(40) Dong, J.; Tang, Y. J.; Nzihou, A.; Weiss-Hortala, E. Effect of steam addition during carbonation, calcination or hydration on reactivation of CaO sorbent for CO2 capture. *J. CO2 Util.* **2020**, *39*, 101167.
(41) Jiang, T.; Zhang, H.; Zhao, Y. J.; Qin, C. L.; Wang, S. P.; Ma, X. B. Kilogram-scale production and pelletization of Al-promoted CaO-based sorbent for CO_2 capture. *Fuel* **2021**, *301*, 121049.
(42) Krodel, M.; Landuyt, A.; Abdala, P. M.; Muller, C. R. Mechanistic Understanding of CaO-Based Sorbents for High-Temperature CO_2 Capture: Advanced Characterization and Prospects. *ChemSusChem* **2020**, *13* (23), 6259−6272.
(43) Hu, Y. C.; Guo, Y. F.; Sun, J.; Li, H. L.; Liu, W. Q. Progress in MgO sorbents for cyclic CO_2 capture: a comprehensive review. *J. Mater. Chem. A* **2019**, *7* (35), 20103−20120.
(44) Huang, C. F.; Xu, M.; Huai, X. L.; Liu, Z. L. Template-Free Synthesis of Hollow CaO/Ca_2SiO_4 Nanoparticle as a Cyclically Stable High-Capacity CO2 Sorbent. *Acs Sustain Chem. Eng.* **2021**, *9* (5), 2171−2179.
(45) Chen, J.; Duan, L. B.; Donat, F.; Muller, C. R. Assessment of the Effect of Process Conditions and Material Characteristics of Alkali Metal Salt Promoted MgO-Based Sorbents on Their CO_2 Capture Performance. *Acs Sustain Chem. Eng.* **2021**, *9* (19), 6659−6672.
(46) Dal Pozzo, A.; Armutlulu, A.; Rekhtina, M.; Abdala, P. M.; Muller, C. R. CO_2 Uptake and Cyclic Stability of MgO-Based CO_2 Sorbents Promoted with Alkali Metal Nitrates and Their Eutectic Mixtures. *Acs Appl. Energ Mater.* **2019**, *2* (2), 1295−1307.
(47) Luzzi, E.; Aprea, P.; Salzano de Luna, M.; Caputo, D.; Filippone, G. Mechanically Coherent Zeolite 13X/Chitosan Aerogel Beads for Effective CO2 Capture. *Acs Appl. Mater. Inter* **2021**, *13* (17), 20728−20734.
(48) Murge, P.; Dinda, S.; Roy, S. Zeolite-Based Sorbent for CO_2 Capture: Preparation and Performance Evaluation. *Langmuir* **2019**, *35* (46), 14751−14760.
(49) Sanna, A.; Maroto-Valer, M. M. CO_2 Capture at High Temperature Using Fly Ash-Derived Sodium Silicates. *Ind. Eng. Chem. Res.* **2016**, *55* (14), 4080−4088.
(50) Vallace, A.; Brooks, S.; Coe, C.; Smith, M. A. Kinetic Model for CO_2 Capture by Lithium Silicates. *J. Phys. Chem. C* **2020**, *124* (37), 20506−20515.
(51) Belgamwar, R.; Maity, A.; Das, T.; Chakraborty, S.; Vinod, C. P.; Polshettiwar, V. Lithium silicate nanosheets with excellent capture capacity and kinetics with unprecedented stability for high-temperature CO2 capture. *Chem. Sci.* **2021**, *12* (13), 4825−4835.
(52) da Silva, I. A.; Mota, C. J. A.Conversion of CO_2 to Light Olefins Over Iron-Based Catalysts Supported on Niobium Oxide. *Front Energy Res.***2019**, *7*. DOI: 10.3389/fenrg.2019.00049
(53) Rodriguez, J. A.; Liu, P.; Stacchiola, D. J.; Senanayake, S. D.; White, M. G.; Chen, J. G. G. Hydrogenation of CO_2 to Methanol: Importance of Metal-Oxide and Metal-Carbide Interfaces in the Activation of CO_2. *ACS Catal.* **2015**, *5* (11), 6696−6706.
(54) Ojelade, O. A.; Zaman, S. F. A review on CO_2 hydrogenation to lower olefins: Understanding the structure-property relationships in heterogeneous catalytic systems. *J. CO2 Util.* **2021**, *47*, 101506.
(55) Siddiqui, M. A. B.; Aitani, A. M.; Saeed, M. R.; Al-Khattaf, S. Enhancing the Production of Light Olefins by Catalytic Cracking of FCC Naphtha over Mesoporous ZSM-5 Catalyst. *Top Catal* **2010**, *53* (19−20), 1387−1393.
(56) Fonseca, N.; dos Santos, L. R. M.; Cerqueira, H. S.; Lemos, F.; Ramoa-Ribeiro, F.; Lam, Y. L.; de Almeida, M. B. B. Olefins production from cracking of a Fischer−Tropsch naphtha. *Fuel* **2012**, *95* (1), 183−189.
(57) Vogt, C.; Knowles, G. P.; Chaffee, A. L. Effect of Syngas Constituents on CdO- and MgO-Based Sorbents for Pre-combustion CO2 Capture. *Energ Fuel* **2015**, *29* (9), 5909−5918.
(58) Peng, J. X.; Iruretagoyena, D.; Chadwick, D. Hydrotalcite/SBA15 composites for pre-combustion CO_2 capture: CO_2 adsorption characteristics. *J. Co2 Util* **2018**, *24*, 73−80.
(59) Zanco, S. E.; Pérez-Calvo, J.-F.; Gasós, A.; Cordiano, B.; Becattini, V.; Mazzotti, M. Postcombustion CO_2 Capture: A Comparative Techno-Economic Assessment of Three Technologies Using a Solvent, an Adsorbent, and a Membrane. *ACS Engineering Au* **2021**, *1* (1), 50−72.
(60) *Oxy-Fuel Combustion for Power Generation and Carbon Dioxide (CO_2) Capture*; Zhang, L., Ed.; Elsevier, 2011.
(61) Wang, X.; Song, C. Carbon Capture From Flue Gas and the Atmosphere: A Perspective. *Front. Energy Res.* **2020**, *8*, 265.
(62) Janajreh, I.; Adeyemi, I.; Raza, S. S.; Ghenai, C. A review of recent developments and future prospects in gasification systems and their modeling. *Renewable and Sustainable Energy Reviews* **2021**, *138*, 110505.
(63) Manzolini, G.; Macchi, E.; Gazzani, M. CO_2 capture in integrated gasification combined cycle with SEWGS-Part B: economic assessment. *Fuel* **2013**, *105*, 220−227.
(64) Song, C.; Pan, W.; Srimat, S. T.; Zheng, J.; Li, Y.; Wang, Y.-H.; Xu, B.-Q.; Zhu, Q.-M. Tri-reforming of methane over Ni catalysts for CO_2 conversion to syngas with desired H_2/CO ratios using flue gas of power plants without CO_2 separation. *Stud. Surf. Sci. Catal.* **2004**, *153*, 315−322.
(65) Xu, X.; Song, C.; Wincek, R.; Andresen, J. M.; Miller, B. G.; Scaroni, A. W. Separation of CO_2 from power plant flue gas using a novel CO_2 "molecular basket" adsorbent. *ACS Fuel Chem. Div. Preprints* **2003**, *48* (1), 162−163.
(66) Dunstan, M. T.; Donat, F.; Bork, A. H.; Grey, C. P.; Müller, C. R. CO_2 capture at medium to high temperature using solid oxide-based sorbents: fundamental aspects, mechanistic insights, and recent advances. *Chem. Rev.* **2021**, *121* (20), 12681−12745.
(67) Yadav, S.; Mondal, S. A review on the progress and prospects of oxy-fuel carbon capture and sequestration (CCS) technology. *Fuel* **2022**, *308*, 122057.
(68) Abuelgasim, S.; Wang, W.; Abdalazeez, A. A brief review for chemical looping combustion as a promising CO_2 capture technology: Fundamentals and progress. *Science of The Total Environment* **2021**, *764*, 142892.
(69) Sanz-Perez, E. S.; Murdock, C. R.; Didas, S. A.; Jones, C. W. Direct Capture of CO_2 from Ambient Air. *Chem. Rev.* **2016**, *116* (19), 11840−11876.
(70) Creamer, A. E.; Gao, B. Carbon-based adsorbents for postcombustion CO_2 capture: a critical review. *Environ. Sci. Technol.* **2016**, *50* (14), 7276−7289.
(71) Li, X.; Xue, Q.; Chang, X.; Zhu, L.; Ling, C.; Zheng, H. Effects of sulfur doping and humidity on CO_2 capture by graphite split pore: a theoretical study. *ACS Appl. Mater. Interfaces* **2017**, *9* (9), 8336−8343.
(72) Luzzi, E.; Aprea, P.; Salzano de Luna, M.; Caputo, D.; Filippone, G. Mechanically Coherent Zeolite 13X/Chitosan Aerogel Beads for Effective CO_2 Capture. *ACS Appl. Mater. Interfaces* **2021**, *13* (17), 20728−20734.
(73) Xing, L.; Wei, K.; Li, Y.; Fang, Z.; Li, Q.; Qi, T.; An, S.; Zhang, S.; Wang, L. TiO_2 Coating Strategy for Robust Catalysis of the Metal-Organic Framework toward Energy-Efficient CO_2 Capture. *Environ. Sci. Technol.* **2021**, *55* (16), 11216−11224.
(74) Nezam, I.; Xie, J.; Golub, K. W.; Carneiro, J.; Olsen, K.; Ping, E. W.; Jones, C. W.; Sakwa-Novak, M. A. Chemical Kinetics of the Autoxidation of Poly (ethylenimine) in CO_2 Sorbents. *ACS Sustainable Chem. Eng.* **2021**, *9* (25), 8477−8486.
(75) Jo, S. B.; Chae, H. J.; Kim, T. Y.; Baek, J.-I.; Ragupathy, D.; Lee, S. C.; Kim, J. C. Thermally stable amine-functionalized silica sorbents using one-pot synthesis method for CO_2 capture at low temperature. *Korean J. Chem. Eng.* **2020**, *37* (12), 2317−2325.
(76) Ünveren, E. E.; Monkul, B. Ö.; Sarıoğlan, Ş.; Karademir, N.; Alper, E. Solid amine sorbents for CO_2 capture by chemical adsorption: A review. *Petroleum* **2017**, *3* (1), 37−50.

(77) Wang, J.; Huang, L.; Yang, R.; Zhang, Z.; Wu, J.; Gao, Y.; Wang, Q.; O'Hare, D.; Zhong, Z. Recent advances in solid sorbents for CO_2 capture and new development trends. *Energy Environ. Sci.* **2014**, *7* (11), 3478−3518.
(78) Samanta, A.; Zhao, A.; Shimizu, G. K.; Sarkar, P.; Gupta, R. Post-combustion CO_2 capture using solid sorbents: a review. *Ind. Eng. Chem. Res.* **2012**, *51* (4), 1438−1463.
(79) Lee, S. C.; Kim, J. C. Dry potassium-based sorbents for CO_2 capture. *Catalysis Surveys from Asia* **2007**, *11* (4), 171−185.
(80) Guo, Y.; Sun, J.; Wang, R.; Li, W.; Zhao, C.; Li, C.; Zhang, J. Recent advances in potassium-based adsorbents for CO_2 capture and separation: a review. *Carbon Capture Science & Technology* **2021**, *1*, 100011.
(81) Rodríguez-Mosqueda, R.; Bramer, E. A.; Roestenberg, T.; Brem, G. Parametrical study on CO_2 capture from ambient air using hydrated K_2CO_3 supported on an activated carbon honeycomb. *Ind. Eng. Chem. Res.* **2018**, *57* (10), 3628−3638.
(82) Veselovskaya, J. V.; Derevschikov, V. S.; Kardash, T. Y.; Stonkus, O. A.; Trubitsina, T. A.; Okunev, A. G. Direct CO_2 capture from ambient air using K_2CO_3/Al_2O_3 composite sorbent. *International Journal of Greenhouse Gas Control* **2013**, *17*, 332−340.
(83) Dong, W.; Chen, X.; Yu, F.; Wu, Y. $Na_2CO_3/MgO/Al_2O_3$ solid sorbents for low-temperature CO_2 capture. *Energy Fuels* **2015**, *29* (2), 968−973.
(84) Won, Y.; Kim, J.-Y.; Park, Y. C.; Yi, C.-K.; Nam, H.; Woo, J.-M.; Jin, G.-T.; Park, J.; Lee, S.-Y.; Jo, S.-H. Post-combustion CO_2 capture process in a circulated fluidized bed reactor using 200 kg potassium-based sorbent: The optimization of regeneration condition. *Energy* **2020**, *208*, 118188.
(85) Zhao, C.; Chen, X.; Zhao, C.; Wu, Y.; Dong, W. K_2CO_3/Al_2O_3 for capturing CO_2 in flue gas from power plants. Part 3: CO_2 capture behaviors of K_2CO_3/Al_2O_3 in a bubbling fluidized-bed reactor. *Energy Fuels* **2012**, *26* (5), 3062−3068.
(86) Prajapati, A.; Renganathan, T.; Krishnaiah, K. Kinetic studies of CO_2 capture using K_2CO_3/activated carbon in fluidized bed reactor. *Energy Fuels* **2016**, *30* (12), 10758−10769.
(87) Qin, Q.; Liu, H.; Zhang, R.; Ling, L.; Fan, M.; Wang, B. Application of density functional theory in studying CO_2 capture with TiO_2-supported K_2CO_3 being an example. *Appl. Energy* **2018**, *231*, 167−178.
(88) Lee, S. C.; Chae, H. J.; Lee, S. J.; Choi, B. Y.; Yi, C. K.; Lee, J. B.; Ryu, C. K.; Kim, J. C. Development of regenerable MgO-based sorbent promoted with K_2CO_3 for CO_2 capture at low temperatures. *Environ. Sci. Technol.* **2008**, *42* (8), 2736−2741.
(89) Li, L.; Li, Y.; Wen, X.; Wang, F.; Zhao, N.; Xiao, F.; Wei, W.; Sun, Y. CO_2 capture over $K_2CO_3/MgO/Al_2O_3$ dry sorbent in a fluidized bed. *Energy Fuels* **2011**, *25* (8), 3835−3842.
(90) Jo, S. B.; Lee, S. C.; Chae, H. J.; Cho, M. S.; Lee, J. B.; Baek, J.-I.; Kim, J. C. Regenerable potassium-based alumina sorbents prepared by CO_2 thermal treatment for post-combustion carbon dioxide capture. *Korean J. Chem. Eng.* **2016**, *33* (11), 3207−3215.
(91) Sengupta, S.; Amte, V.; Dongara, R.; Das, A. K.; Bhunia, H.; Bajpai, P. K. Effects of the adsorbent preparation method for CO_2 capture from flue gas using K_2CO_3/Al_2O_3 adsorbents. *Energy Fuels* **2015**, *29* (1), 287−297.
(92) Zhao, C.; Chen, X.; Zhao, C. Multiple-cycles behavior of K_2CO_3/Al_2O_3 for CO_2 capture in a fluidized-bed reactor. *Energy Fuels* **2010**, *24* (2), 1009−1012.
(93) Cho, M. S.; Lee, S. C.; Chae, H. J.; Kwon, Y. M.; Lee, J. B.; Kim, J. C. Characterization of new potassium-based solid sorbents prepared using metal silicates for post-combustion CO_2 capture. *Process Saf. Environ. Prot.* **2018**, *117*, 296−306.
(94) Lee, S. C.; Chae, H. J.; Choi, B. Y.; Jung, S. Y.; Ryu, C. Y.; Park, J. J.; Baek, J.-I.; Ryu, C. K.; Kim, J. C. The effect of relative humidity on CO_2 capture capacity of potassium-based sorbents. *Korean J. Chem. Eng.* **2011**, *28* (2), 480−486.
(95) Lee, S. C.; Choi, B. Y.; Ryu, C. K.; Ahn, Y. S.; Lee, T. J.; Kim, J. C. The effect of water on the activation and the CO_2 capture capacities of alkali metal-based sorbents. *Korean J. Chem. Eng.* **2006**, *23* (3), 374−379.
(96) Duan, Y.; Luebke, D. R.; Pennline, H. W.; Li, B.; Janik, M. J.; Halley, J. W. Ab initio thermodynamic study of the CO_2 capture properties of potassium carbonate sesquihydrate, $K_2CO_3 \cdot 1.5\ H_2O$. *J. Phys. Chem. C* **2012**, *116* (27), 14461−14470.
(97) Liu, M.; Vogt, C.; Chaffee, A. L.; Chang, S. L. Nanoscale structural investigation of Cs_2CO_3-doped MgO sorbent for CO_2 capture at moderate temperature. *J. Phys. Chem. C* **2013**, *117* (34), 17514−17520.
(98) Hu, Y.; Guo, Y.; Sun, J.; Li, H.; Liu, W. Progress in MgO sorbents for cyclic CO_2 capture: a comprehensive review. *Journal of Materials Chemistry A* **2019**, *7* (35), 20103−20120.
(99) Ruhaimi, A.; Aziz, M.; Jalil, A. Magnesium oxide-based adsorbents for carbon dioxide capture: Current progress and future opportunities. *Journal of CO2 Utilization* **2021**, *43*, 101357.
(100) Gao, W.; Vasiliades, M. A.; Damaskinos, C. M.; Zhao, M.; Fan, W.; Wang, Q.; Reina, T. R.; Efstathiou, A. M. Molten Salt-Promoted MgO Adsorbents for CO_2 Capture: Transient Kinetic Studies. *Environ. Sci. Technol.* **2021**, *55* (8), 4513−4521.
(101) Yang, Y.; Chen, K.; Huang, L.; Li, M.; Zhang, T.; Zhong, M.; Ning, P.; Wang, J.; Wen, S. Research on $Li_{0.3}Na_{0.18}K_{0.52}NO_3$ promoted $Mg_{20}Al\text{-}CO_3$ LDH/GO composites for CO_2 capture. *Journal of Industrial and Engineering Chemistry* **2021**, *102*, 86−94.
(102) Zhao, X.; Ji, G.; Liu, W.; He, X.; Anthony, E. J.; Zhao, M. Mesoporous MgO promoted with $NaNO_3/NaNO_2$ for rapid and high-capacity CO_2 capture at moderate temperatures. *Chem. Eng. J.* **2018**, *332*, 216−226.
(103) Harada, T.; Simeon, F.; Hamad, E. Z.; Hatton, T. A. Alkali metal nitrate-promoted high-capacity MgO adsorbents for regenerable CO_2 capture at moderate temperatures. *Chem. Mater.* **2015**, *27* (6), 1943−1949.
(104) Bukhtiyarova, M. A review on effect of synthesis conditions on the formation of layered double hydroxides. *J. Solid State Chem.* **2019**, *269*, 494−506.
(105) Manohara, G.; Norris, D.; Maroto-Valer, M. M.; Garcia, S. Acetate intercalated Mg-Al layered double hydroxides (LDHs) through modified amide hydrolysis: a new route to synthesize novel mixed metal oxides (MMOs) for CO_2 capture. *Dalton Transactions* **2021**, *50* (21), 7474−7483.
(106) Veerabhadrappa, M. G.; Maroto-Valer, M. M.; Chen, Y.; Garcia, S. Layered Double Hydroxides-Based Mixed Metal Oxides: Development of Novel Structured Sorbents for CO_2 Capture Applications. *ACS Appl. Mater. Interfaces* **2021**, *13* (10), 11805−11813.
(107) Faramawy, S.; Zaki, T.; Sakr, A.-E.; Saber, O.; Aboul-Gheit, A.; Hassan, S. The activity of Mg-Al layered double hydroxides intercalated with nitrogen-containing anions towards the removal of carbon dioxide from natural gas. *Journal of Natural Gas Science and Engineering* **2018**, *54*, 72−82.
(108) Naeem, M. A.; Armutlulu, A.; Imtiaz, Q.; Donat, F.; Schäublin, R.; Kierzkowska, A.; Müller, C. R. Optimization of the structural characteristics of CaO and its effective stabilization yield high-capacity CO_2 sorbents. *Nat. Commun.* **2018**, *9* (1), 1−11.
(109) Erans, M.; Manovic, V.; Anthony, E. J. Calcium looping sorbents for CO_2 capture. *Appl. Energy* **2016**, *180*, 722−742.
(110) Tian, S.; Jiang, J.; Zhang, Z.; Manovic, V. Inherent potential of steelmaking to contribute to decarbonisation targets via industrial carbon capture and storage. *Nat. Commun.* **2018**, *9* (1), 1−8.
(111) Hanak, D. P.; Biliyok, C.; Manovic, V. Calcium looping with inherent energy storage for decarbonisation of coal-fired power plant. *Energy Environ. Sci.* **2016**, *9* (3), 971−983.
(112) Yoon, H. J.; Lee, K. B. Introduction of chemically bonded zirconium oxide in CaO-based high-temperature CO_2 sorbents for enhanced cyclic sorption. *Chem. Eng. J.* **2019**, *355*, 850−857.
(113) Sun, H.; Wu, C.; Shen, B.; Zhang, X.; Zhang, Y.; Huang, J. Progress in the development and application of CaO-based adsorbents for CO_2 capture—a review. *Materials Today Sustainability* **2018**, *1*, 1−27.

(114) Krödel, M.; Landuyt, A.; Abdala, P. M.; Müller, C. R. Mechanistic Understanding of CaO-Based Sorbents for High-Temperature CO_2 Capture: Advanced Characterization and Prospects. *ChemSusChem* **2020**, *13* (23), 6259.
(115) Hu, Y.; Lu, H.; Liu, W.; Yang, Y.; Li, H. Incorporation of CaO into inert supports for enhanced CO_2 capture: A review. *Chem. Eng. J.* **2020**, *396*, 125253.
(116) Al-Mamoori, A.; Lawson, S.; Rownaghi, A. A.; Rezaei, F. Improving adsorptive performance of CaO for high-temperature CO_2 capture through Fe and Ga doping. *Energy Fuels* **2019**, *33* (2), 1404−1413.
(117) Zhang, L.; Zhang, B.; Yang, Z.; Guo, M. The Role of Water on the Performance of Calcium Oxide-Based Sorbents for Carbon Dioxide Capture: A Review. *Energy technology* **2015**, *3* (1), 10−19.
(118) Jia, L.; Hughes, R.; Lu, D.; Anthony, E.; Lau, I. Attrition of calcining limestones in circulating fluidized-bed systems. *Ind. Eng. Chem. Res.* **2007**, *46* (15), 5199−5209.
(119) Manovic, V.; Anthony, E. J. Screening of binders for pelletization of CaO-based sorbents for CO_2 capture. *Energy Fuels* **2009**, *23* (10), 4797−4804.
(120) Chen, H.; Zhao, C.; Yang, Y. Enhancement of attrition resistance and cyclic CO_2 capture of calcium-based sorbent pellets. *Fuel Process. Technol.* **2013**, *116*, 116−122.
(121) Zhang, Y.; Gao, Y.; Pfeiffer, H.; Louis, B.; Sun, L.; O'Hare, D.; Wang, Q. Recent advances in lithium containing ceramic based sorbents for high-temperature CO_2 capture. *Journal of Materials Chemistry A* **2019**, *7* (14), 7962−8005.
(122) Yan, X.; Li, Y.; Ma, X.; Zhao, J.; Wang, Z. Performance of Li_4SiO_4 material for CO_2 capture: a review. *Int. J. Mol. Sci.* **2019**, *20* (4), 928.
(123) Li, F.; Wang, Y.; Liu, K.; Wu, Y.; Ai, J.; Zhang, J. Preparation of Li_4SiO_4-based adsorbents with coal slag for high temperature cyclic CO_2 capture. *Fuel* **2022**, *310*, 121687.
(124) Wang, J.; Zhang, T.; Yang, Y.; Li, M.; Qin, Q.; Lu, P.; Ning, P.; Wang, Q. Unexpected highly reversible lithium-silicate-based CO_2 sorbents derived from sediment of Dianchi Lake. *Energy Fuels* **2019**, *33* (3), 1734−1744.
(125) Belgamwar, R.; Maity, A.; Das, T.; Chakraborty, S.; Vinod, C. P.; Polshettiwar, V. Lithium silicate nanosheets with excellent capture capacity and kinetics with unprecedented stability for high-temperature CO_2 capture. *Chemical Science* **2021**, *12* (13), 4825−4835.
(126) Seggiani, M.; Puccini, M.; Vitolo, S. Alkali promoted lithium orthosilicate for CO_2 capture at high temperature and low concentration. *International Journal of Greenhouse Gas Control* **2013**, *17*, 25−31.
(127) Subha, P.; Nair, B. N.; Mohamed, A. P.; Anilkumar, G.; Warrier, K.; Yamaguchi, T.; Hareesh, U. Morphologically and compositionally tuned lithium silicate nanorods as high-performance carbon dioxide sorbents. *Journal of Materials Chemistry A* **2016**, *4* (43), 16928−16935.
(128) Yang, X.; Liu, W.; Sun, J.; Hu, Y.; Wang, W.; Chen, H.; Zhang, Y.; Li, X.; Xu, M. Alkali-Doped Lithium Orthosilicate Sorbents for Carbon Dioxide Capture. *ChemSusChem* **2016**, *9* (17), 2480−2487.
(129) Kwon, Y. M.; Chae, H. J.; Cho, M. S.; Park, Y. K.; Seo, H. M.; Lee, S. C.; Kim, J. C. Effect of a Li_2SiO_3 phase in lithium silicate-based sorbents for CO_2 capture at high temperatures. *Sep. Purif. Technol.* **2019**, *214*, 104−110.
(130) Lee, S. C.; Kim, M. J.; Kwon, Y. M.; Chae, H. J.; Cho, M. S.; Park, Y. K.; Seo, H. M.; Kim, J. C. Novel regenerable solid sorbents based on lithium orthosilicate for carbon dioxide capture at high temperatures. *Sep. Purif. Technol.* **2019**, *214*, 120−127.
(131) Kim, H.; Jang, H. D.; Choi, M. Facile synthesis of macroporous Li_4SiO_4 with remarkably enhanced CO_2 adsorption kinetics. *Chem. Eng. J.* **2015**, *280*, 132−137.
(132) Subha, P.; Nair, B. N.; Hareesh, P.; Mohamed, A. P.; Yamaguchi, T.; Warrier, K.; Hareesh, U. Enhanced CO_2 absorption kinetics in lithium silicate platelets synthesized by a sol-gel approach. *Journal of Materials Chemistry A* **2014**, *2* (32), 12792−12798.
(133) Zimmermann, H.Light olefins-challenges from new production routes?*DGMK/SCI-Conference*; Hamburg, Germany, October 10−12, 2007.
(134) Zhao, Z.; Jiang, J.; Wang, F. An economic analysis of twenty light olefin production pathways. *Journal of Energy Chemistry* **2021**, *56*, 193−202.
(135) Gholami, Z.; Gholami, F.; Tišler, Z.; Tomas, M.; Vakili, M. A Review on Production of Light Olefins via Fluid Catalytic Cracking. *Energies* **2021**, *14* (4), 1089.
(136) Amghizar, I.; Vandewalle, L. A.; Van Geem, K. M.; Marin, G. B. New trends in olefin production. *Engineering* **2017**, *3* (2), 171−178.
(137) Bahmanpour, A. M.; Héroguel, F.; Kılıç, M.; Baranowski, C. J.; Artiglia, L.; Röthlisberger, U.; Luterbacher, J. S.; Kröcher, O. Cu-Al Spinel as a Highly Active and Stable Catalyst for the Reverse Water Gas Shift Reaction. *ACS Catal.* **2019**, *9* (7), 6243−6251.
(138) Wang, J.; Liu, C.-Y.; Senftle, T. P.; Zhu, J.; Zhang, G.; Guo, X.; Song, C. Variation in the In_2O_3 Crystal Phase Alters Catalytic Performance toward the Reverse Water Gas Shift Reaction. *ACS Catal.* **2020**, *10* (5), 3264−3273.
(139) Gu, M.; Dai, S.; Qiu, R.; Ford, M. E.; Cao, C.; Wachs, I. E.; Zhu, M. Structure-Activity Relationships of Copper- and Potassium-Modified Iron Oxide Catalysts during Reverse Water-Gas Shift Reaction. *ACS Catal.* **2021**, *11* (20), 12609−12619.
(140) Vovchok, D.; Zhang, C.; Hwang, S.; Jiao, L.; Zhang, F.; Liu, Z.; Senanayake, S. D.; Rodriguez, J. A. Deciphering Dynamic Structural and Mechanistic Complexity in Cu/CeO_2/ZSM-5 Catalysts for the Reverse Water-Gas Shift Reaction. *ACS Catal.* **2020**, *10* (17), 10216−10228.
(141) Wambach, J.; Baiker, A.; Wokaun, A. CO_2 hydrogenation over metal/zirconia catalysts CO. *Phys. Chem. Chem. Phys.* **1999**, *1* (22), 5071−5080.
(142) Kattel, S.; Yan, B. H.; Chen, J. G. G.; Liu, P. CO_2 hydrogenation on Pt, $PtiSiO_2$ and Pt/TiO_2: Importance of synergy between Pt and oxide support. *J. Catal.* **2016**, *343*, 115−126.
(143) Sakurai, H.; Tsubota, S.; Haruta, M. Hydrogenation of CO_2 over Gold Supported on Metal-Oxides. *Appl. Catal. a-Gen* **1993**, *102* (2), 125−136.
(144) Porosoff, M. D.; Chen, J. G. G. Trends in the catalytic reduction of CO_2 by hydrogen over supported monometallic and bimetallic catalysts. *J. Catal.* **2013**, *301*, 30−37.
(145) Aitbekova, A.; Wu, L. H.; Wrasman, C. J.; Boubnov, A.; Hoffman, A. S.; Goodman, E. D.; Bare, S. R.; Cargnello, M. Low-Temperature Restructuring of CeO_2-Supported Ru Nanoparticles Determines Selectivity in CO_2 Catalytic Reduction. *J. Am. Chem. Soc.* **2018**, *140* (42), 13736−13745.
(146) Davis, B. H. Fischer−Tropsch synthesis: current mechanism and futuristic needs. *Fuel Process. Technol.* **2001**, *71* (1−3), 157−166.
(147) de Smit, E.; Weckhuysen, B. M. The renaissance of iron-based Fischer−Tropsch synthesis: on the multifaceted catalyst deactivation behaviour. *Chem. Soc. Rev.* **2008**, *37* (12), 2758−2781.
(148) Bell, A. T. Catalytic Synthesis of Hydrocarbons over Group-Viii Metals - a Discussion of the Reaction-Mechanism. *Catal. Rev.* **1981**, *23* (1−2), 203−232.
(149) Torres Galvis, H. M.; de Jong, K. P. Catalysts for Production of Lower Olefins from Synthesis Gas: A Review. *ACS Catal.* **2013**, *3* (9), 2130−2149.
(150) Chaumette, P.; Courty, P.; Kiennemann, A.; Ernst, B. Higher Alcohol and Paraffin Synthesis on Cobalt-Based Catalysts - Comparison of Mechanistic Aspects. *Top Catal* **1995**, *2* (1−4), 117−126.
(151) Choi, Y. H.; Ra, E. C.; Kim, E. H.; Kim, K. Y.; Jang, Y. J.; Kang, K. N.; Choi, S. H.; Jang, J. H.; Lee, J. S. Sodium-Containing Spinel Zinc Ferrite as a Catalyst Precursor for the Selective Synthesis of Liquid Hydrocarbon Fuels. *ChemSusChem* **2017**, *10* (23), 4764−4770.
(152) Xie, J.; Yang, J.; Dugulan, A. I.; Holmen, A.; Chen, D.; de Jong, K. P.; Louwerse, M. J. Size and Promoter Effects in Supported Iron Fischer−Tropsch Catalysts: Insights from Experiment and Theory. *ACS Catal.* **2016**, *6* (5), 3147−3157.

https://doi.org/10.1021/acscatal.2c01646
ACS Catal. 2022, 12, 7486−7510

(153) Cheng, Y.; Lin, J.; Xu, K.; Wang, H.; Yao, X. Y.; Pei, Y.; Yan, S. R.; Qiao, M. H.; Zong, B. N. Fischer−Tropsch Synthesis to Lower Olefins over Potassium-Promoted Reduced Graphene Oxide Supported Iron Catalysts. *ACS Catal.* **2016**, *6* (1), 389−399.

(154) Ma, Z. Z.; Ma, H. F.; Zhang, H. T.; Wu, X.; Qian, W. X.; Sun, Q. W.; Ying, W. Y. Direct Conversion of Syngas to Light Olefins through Fischer- Tropsch Synthesis over Fe-Zr Catalysts Modified with Sodium. *Acs Omega* **2021**, *6* (7), 4968−4976.

(155) Han, Z. H.; Qian, W. X.; Zhang, H. T.; Ma, H. F.; Sun, Q. W.; Ying, W. Y. Effect of Rare-Earth Promoters on Precipitated Iron-Based Catalysts for Fischer−Tropsch Synthesis. *Ind. Eng. Chem. Res.* **2020**, *59* (33), 14598−14605.

(156) Ismail, A. S. M.; Casavola, M.; Liu, B. Y.; Gloter, A.; van Deelen, T. W.; Versluijs, M.; Meeldijk, J. D.; Stephan, O.; de Jong, K. P.; de Groot, F. M. F. Atomic-Scale Investigation of the Structural and Electronic Properties of Cobalt-Iron Bimetallic Fischer−Tropsch Catalysts. *ACS Catal.* **2019**, *9* (9), 7998−8011.

(157) Hernandez Mejia, C.; van der Hoeven, J. E. S.; de Jongh, P. E.; de Jong, K. P. Cobalt-Nickel Nanoparticles Supported on Reducible Oxides as Fischer−Tropsch Catalysts. *ACS Catal.* **2020**, *10* (13), 7343−7354.

(158) Tian, H.; Li, X. Y.; Zeng, L.; Gong, J. L. Recent Advances on the Design of Group VIII Base-Metal Catalysts with Encapsulated Structures. *ACS Catal.* **2015**, *5* (8), 4959−4977.

(159) Aramouni, N. A. K.; Touma, J. G.; Tarboush, B. A.; Zeaiter, J.; Ahmad, M. N. Catalyst design for dry reforming of methane: Analysis review. *Renew Sust Energ Rev.* **2018**, *82*, 2570−2585.

(160) Freund, H. J.; Messmer, R. P. On the Bonding and Reactivity of CO_2 on Metal-Surfaces. *Surf. Sci.* **1986**, *172* (1), 1−30.

(161) Jang, W. J.; Shim, J. O.; Kim, H. M.; Yoo, S. Y.; Roh, H. S. A review on dry reforming of methane in aspect of catalytic properties. *Catal. Today* **2019**, *324*, 15−26.

(162) Hou, Z. Y.; Chen, P.; Fang, H. L.; Zheng, X. M.; Yashima, T. Production of synthesis gas via methane reforming with CO_2 on noble metals and small amount of noble-(Rh-) promoted Ni catalysts. *Int. J. Hydrogen Energ* **2006**, *31* (5), 555−561.

(163) Castro Luna, A. E.; Iriarte, M. E. Carbon dioxide reforming of methane over a metal modified Ni-Al_2O_3 catalyst. *Appl. Catal. a-Gen* **2008**, *343* (1−2), 10−15.

(164) Therdthianwong, S.; Siangchin, C.; Therdthianwong, A. Improvement of coke resistance of Ni/Al_2O_3 catalyst in CH_4/CO_2 reforming by ZrO_2 addition. *Fuel Process. Technol.* **2008**, *89* (2), 160−168.

(165) Tomiyama, S.; Takahashi, R.; Sato, S.; Sodesawa, T.; Yoshida, S. Preparation of Ni/SiO_2 catalyst with high thermal stability for CO_2-reforming of CH4. *Appl. Catal. a-Gen* **2003**, *241* (1−2), 349−361.

(166) Zeng, S. H.; Zhang, L.; Zhang, X. H.; Wang, Y.; Pan, H.; Su, H. Q. Modification effect of natural mixed rare earths on Co/gamma-Al_2O_3 catalysts for CH_4/CO_2 reforming to synthesis gas. *Int. J. Hydrogen Energ* **2012**, *37* (13), 9994−10001.

(167) Mette, K.; Kuhl, S.; Tarasov, A.; Willinger, M. G.; Krohnert, J.; Wrabetz, S.; Trunschke, A.; Scherzer, M.; Girgsdies, F.; Dudder, H.; Kahler, K.; Ortega, K. F.; Muhler, M.; Schlogl, R.; Behrens, M.; Lunkenbein, T. High-Temperature Stable Ni Nanoparticles for the Dry Reforming of Methane. *ACS Catal.* **2016**, *6* (10), 7238−7248.

(168) Ferreira-Aparicio, P.; Rodriguez-Ramos, I.; Anderson, J. A.; Guerrero-Ruiz, A. Mechanistic aspects of the dry reforming of methane over ruthenium catalysts. *Appl. Catal. a-Gen* **2000**, *202* (2), 183−196.

(169) Al-Fatesh, A. S.; Kumar, R.; Kasim, S. O.; Ibrahim, A. A.; Fakeeha, A. H.; Abasaeed, A. E.; Alrasheed, R.; Bagabas, A.; Chaudhary, M. L.; Frusteri, F.; Chowdhury, B. The effect of modifier identity on the performance of Ni-based catalyst supported on gamma-Al_2O_3 in dry reforming of methane. *Catal. Today* **2020**, *348*, 236−242.

(170) Sokolov, S.; Kondratenko, E. V.; Pohl, M. M.; Barkschat, A.; Rodemerck, U. Stable low-temperature dry reforming of methane over mesoporous La_2O_3-ZrO_2 supported Ni catalyst. *Appl. Catal. B-Environ* **2012**, *113*, 19−30.

(171) El Hassan, N.; Kaydouh, M. N.; Geagea, H.; El Zein, H.; Jabbour, K.; Casale, S.; El Zakhem, H.; Massiani, P. Low temperature dry reforming of methane on rhodium and cobalt based catalysts: Active phase stabilization by confinement in mesoporous SBA-15. *Appl. Catal. a-Gen* **2016**, *520*, 114−121.

(172) Zhang, M. L.; Ji, S. F.; Hu, L. H.; Yin, F. X.; Li, C. Y.; Liu, H. Structural characterization of highly stable Ni/SBA-15 catalyst and its catalytic performance for methane reforming with CO_2. *Chinese J. Catal* **2006**, *27* (9), 777−782.

(173) Abdulrasheed, A.; Jalil, A. A.; Gambo, Y.; Ibrahim, M.; Hambali, H. U.; Shahul Hamid, M. Y. A review on catalyst development for dry reforming of methane to syngas: Recent advances. *Renew Sust Energ Rev.* **2019**, *108*, 175−193.

(174) Das, S.; Sengupta, M.; Patel, J.; Bordoloi, A. A study of the synergy between support surface properties and catalyst deactivation for CO_2 reforming over supported Ni nanoparticles. *Appl. Catal. a-Gen* **2017**, *545*, 113−126.

(175) Wang, S. B.; Lu, G. Q. M.; Millar, G. J. Carbon dioxide reforming of methane to produce synthesis gas over metal-supported catalysts: State of the art. *Energ Fuel* **1996**, *10* (4), 896−904.

(176) Gadalla, A. M.; Bower, B. The Role of Catalyst Support on the Activity of Nickel for Reforming Methane with CO_2. *Chem. Eng. Sci.* **1988**, *43* (11), 3049−3062.

(177) Sutthiumporn, K.; Maneerung, T.; Kathiraser, Y.; Kawi, S. CO_2 dry-reforming of methane over $La_{0.8}Sr_{0.2}Ni_{0.8}M_{0.2}O_3$ perovskite (M = Bi, Co, Cr, Cu, Fe): Roles of lattice oxygen on C-H activation and carbon suppression. *Int. J. Hydrogen Energ* **2012**, *37* (15), 11195−11207.

(178) Gallego, G. S.; Mondragon, F.; Barrault, J.; Tatibouet, J. M.; Batiot-Dupeyrat, C. CO_2 reforming of CH_4 over La-Ni based perovskite precursors. *Appl. Catal. a-Gen* **2006**, *311*, 164−171.

(179) Pereniguez, R.; Gonzalez-DelaCruz, V. M.; Holgado, J. P.; Caballero, A. Synthesis and characterization of a $LaNiO_3$ perovskite as precursor for methane reforming reactions catalysts. *Appl. Catal. B-Environ* **2010**, *93* (3−4), 346−353.

(180) Arandiyan, H.; Peng, Y.; Liu, C. X.; Chang, H. Z.; Li, J. H. Effects of noble metals doped on mesoporous LaAlNi mixed oxide catalyst and identification of carbon deposit for reforming CH_4 with CO_2. *J. Chem. Technol. Biot* **2014**, *89* (3), 372−381.

(181) Shah, S.; Sayono, S.; Ynzunza, J.; Pan, R.; Xu, M. J.; Pan, X. Q.; Gilliard-AbdulAziz, K. L.The effects of stoichiometry on the properties of exsolved Ni-Fe alloy nanoparticles for dry methane reforming. *AIChE J.***2020**, *66* (12). DOI: 10.1002/aic.17078

(182) Shah, S.; Xu, M. J.; Pan, X. Q.; Gilliard-Abdulaziz, K. L. Exsolution of Embedded Ni-Fe-Co Nanoparticles: Implications for Dry Reforming of Methane. *Acs Appl. Nano Mater.* **2021**, *4* (8), 8626−8636.

(183) Zhang, J. G.; Wang, H.; Dalai, A. K. Development of stable bimetallic catalysts for carbon dioxide reforming of methane. *J. Catal.* **2007**, *249* (2), 300−310.

(184) Wang, W. Y.; Wang, G. C. Nickel/Molybdenum Bimetallic Alloy for Dry Reforming of Methane: A Coverage-Dependence Microkinetic Model Simulation Based on the First-Principles Calculation. *J. Phys. Chem. C* **2021**, *125* (34), 18653−18664.

(185) Turap, Y.; Wang, I.; Fu, T. T.; Wu, Y. M.; Wang, Y. D.; Wang, W. Co-Ni alloy supported on CeO_2 as a bimetallic catalyst for dry reforming of methane. *Int. J. Hydrogen Energ* **2020**, *45* (11), 6538−6548.

(186) Campanati, M.; Fornasari, G.; Vaccari, A. Fundamentals in the preparation of heterogeneous catalysts. *Catal. Today* **2003**, *77* (4), 299−314.

(187) Zeng, S.; Zhang, L.; Zhang, X.; Wang, Y.; Pan, H.; Su, H. Modification effect of natural mixed rare earths on Co/γ-Al_2O_3 catalysts for CH_4/CO_2 reforming to synthesis gas. *Int. J. Hydrogen Energ* **2012**, *37* (13), 9994−10001.

(188) Jeong, H.; Kim, K. I.; Kim, D.; Song, I. K. Effect of promoters in the methane reforming with carbon dioxide to synthesis gas over Ni/HY catalysts. *J. Mol. Catal. a-Chem.* **2006**, *246* (1−2), 43−48.

(189) San Jose-Alonso, D.; Illan-Gomez, M. J.; Roman-Martinez, M. C. K and Sr promoted Co alumina supported catalysts for the CO_2 reforming of methane. *Catal. Today* **2011**, *176* (1), 187−190.

(190) Olah, G. A.; Goeppert, A.; Prakash, G. K. S. Chemical Recycling of Carbon Dioxide to Methanol and Dimethyl Ether: From Greenhouse Gas to Renewable, Environmentally Carbon Neutral Fuels and Synthetic Hydrocarbons. *Journal of Organic Chemistry* **2009**, *74* (2), 487−498.
(191) Olah, G. A.; Prakash, G. K. S.; Goeppert, A. Anthropogenic Chemical Carbon Cycle for a Sustainable Future. *J. Am. Chem. Soc.* **2011**, *133* (33), 12881−12898.
(192) Ohyama, S. Low-temperature methanol synthesis in catalytic systems composed of nickel compounds and alkali alkoxides in liquid phases. *Appl. Catal. a-Gen* **1999**, *180* (1−2), 217−225.
(193) Grabow, L. C.; Mavrikakis, M. Mechanism of Methanol Synthesis on Cu through CO_2 and CO Hydrogenation. *ACS Catal.* **2011**, *1* (4), 365−384.
(194) Studt, F.; Abild-Pedersen, F.; Wu, Q. X.; Jensen, A. D.; Temel, B.; Grunwaldt, J. D.; Norskov, J. K. CO hydrogenation to methanol on Cu-Ni catalysts: Theory and experiment. *J. Catal.* **2012**, *293*, 51−60.
(195) Ashwell, A. P.; Lin, W.; Hofman, M. S.; Yang, Y. X.; Ratner, M. A.; Koel, B. E.; Schatz, G. C. Hydrogenation of CO to Methanol on Ni(110) through Subsurface Hydrogen. *J. Am. Chem. Soc.* **2017**, *139* (48), 17582−17589.
(196) Docherty, S. R.; Phongprueksathat, N.; Lam, E.; Noh, G.; Safonova, O. V.; Urakawa, A.; Copéret, C. Silica-Supported PdGa Nanoparticles: Metal Synergy for Highly Active and Selective CO_2-to-CH_3OH Hydrogenation. *JACS Au* **2021**, *1* (4), 450−458.
(197) Koizumi, N.; Jiang, X.; Kugai, J.; Song, C. Effects of mesoporous silica supports and alkaline promoters on activity of Pd catalysts in CO_2 hydrogenation for methanol synthesis. *Catal. Today* **2012**, *194* (1), 16−24.
(198) Zou, T.; Araújo, T. P.; Krumeich, F.; Mondelli, C.; Pérez-Ramírez, J. ZnO-Promoted Inverse ZrO_2-Cu Catalysts for CO_2-Based Methanol Synthesis under Mild Conditions. *Acs Sustain Chem. Eng.* **2022**, *10* (1), 81−90.
(199) Kim, H.; Lee, S.; Jang, S.; Yu, J. H.; Yoo, J. S.; Oh, J. Effect of facile nitrogen doping on catalytic performance of NaW/Mn/SiO_2 for oxidative coupling of methane. *Appl. Catal. B-Environ* **2021**, *292*, 120161.
(200) Kwon, D.; Yang, I.; An, S.; Cho, J.; Ha, J.-M.; Jung, J. C. A study on active sites of A_2BO_4 catalysts with perovskite-like structures in oxidative coupling of methane. *Molecular Catalysis* **2021**, *506*, 111548.
(201) Xu, Y. D.; Yu, L.; Cai, C.; Huang, J. S.; Guo, X. X. A Study of the Oxidative Coupling of Methane over Sro-La_2O_3/Cao Catalysts by Using CO_2 as a Probe. *Catal. Lett.* **1995**, *35* (3−4), 215−231.
(202) Zhang, Y. Z.; Cho, Y. H.; Yamaguchi, A.; Peng, X. B.; Miyauchi, M.; Abe, H.; Fujita, T. CO_2 oxidative coupling of methane using an earth-abundant CaO-based catalyst. *Sci. Rep.* **2019**, *9*, 15454.
(203) Lunsford, J. H. The Catalytic Oxidative Coupling of Methane. *Angew. Chem., Int. Ed. Engl.* **1995**, *34* (9), 970−980.
(204) Arinaga, A. M.; Ziegelski, M. C.; Marks, T. J. Alternative Oxidants for the Catalytic Oxidative Coupling of Methane. *Angew. Chem.* **2021**, *133* (19), 10596−10609.
(205) Yoon, S.; Lim, S.; Choi, J.-W.; Suh, D. J.; Song, K. H.; Ha, J.-M. Study on the unsteady state oxidative coupling of methane: effects of oxygen species from O_2, surface lattice oxygen, and CO_2 on the C^{2+} selectivity. *RSC Adv.* **2020**, *10* (59), 35889−35897.
(206) Xu, Y.; Yu, L.; Cai, C.; Huang, J.; Guo, X. A study of the oxidative coupling of methane over SrO-La_2O_3/CaO catalysts by using CO_2 as a probe. *Catalysis letters* **1995**, *35* (3), 215−231.
(207) Shi, J.; Yao, L.; Hu, C. Effect of CO2 on the structural variation of Na_2WO_4/Mn/SiO_2 catalyst for oxidative coupling of methane to ethylene. *Journal of energy chemistry* **2015**, *24* (4), 394−400.
(208) Nishiyama, T.; Aika, K.-I. Mechanism of the oxidative coupling of methane using CO_2 as an oxidant over PbO/ MgO. *J. Catal.* **1990**, *122* (2), 346−351.
(209) Suzuki, T.; Wada, K.; Watanabe, Y. Effects of carbon dioxide and catalyst preparation on the oxidative dimerization of methane. *Applied catalysis* **1990**, *59* (1), 213−225.
(210) Chen, C.; Xu, Y.; Li, G.; Guo, X. Oxidative coupling of methane by carbon dioxide: a highly C_2 selective La_2O_3/ZnO catalyst. *Catalysis letters* **1996**, *42* (3), 149−153.
(211) Korf, S. J.; Roos, J. A.; de Bruijn, N. A.; van Ommen, J. G.; Ross, J. R. Influence of CO_2 on the oxidative coupling of methane over a lithium promoted magnesium oxide catalyst. *J. Chem. Soc., Chem. Commun.* **1987**, No. 19, 1433−1434.
(212) Smith, K. J.; Galuszka, J. Effect of carbon dioxide on methane oxidative coupling kinetics. *Ind. Eng. Chem. Res.* **1994**, *33* (1), 14−20.
(213) Ashok, J.; Pati, S.; Hongmanorom, P.; Tianxi, Z.; Junmei, C.; Kawi, S. A review of recent catalyst advances in CO_2 methanation processes. *Catal. Today* **2020**, *356*, 471−489.
(214) Salehi, J.; Namvar, A.; Gazijahani, F. S.; Shafie-khah, M.; Catalão, J. P. Effect of power-to-gas technology in energy hub optimal operation and gas network congestion reduction. *Energy* **2022**, *240*, 122835.
(215) Momeni, M.; Soltani, M.; Hosseinpour, M.; Nathwani, J. A comprehensive analysis of a power-to-gas energy storage unit utilizing captured carbon dioxide as a raw material in a large-scale power plant. *Energy Convers. Manage.* **2021**, *227*, 113613.
(216) Gotz, M.; Lefebvre, J.; Mors, F.; McDaniel Koch, A.; Graf, F.; Bajohr, S.; Reimert, R.; Kolb, T. Renewable Power-to-Gas: A technological and economic review. *Renewable Energy* **2016**, *85*, 1371−1390.
(217) Ikäheimo, J.; Weiss, R.; Kiviluoma, J.; Pursiheimo, E.; Lindroos, T. J. Impact of power-to-gas on the cost and design of the future low-carbon urban energy system. *Appl. Energy* **2022**, *305*, 117713.
(218) Lv, C.; Xu, L.; Chen, M.; Cui, Y.; Wen, X.; Li, Y.; Wu, C.-e; Yang, B.; Miao, Z.; Hu, X.; Shou, Q. Recent progresses in constructing the highly efficient Ni based catalysts with advanced low-temperature activity toward CO_2 methanation. *Front. Chem.* **2020**, *8*, 269.
(219) Muroyama, H.; Tsuda, Y.; Asakoshi, T.; Masitah, H.; Okanishi, T.; Matsui, T.; Eguchi, K. Carbon dioxide methanation over Ni catalysts supported on various metal oxides. *J. Catal.* **2016**, *343*, 178−184.
(220) Wang, X.; Zhu, L.; Zhuo, Y.; Zhu, Y.; Wang, S. Enhancement of CO_2 methanation over La-modified Ni/SBA-15 catalysts prepared by different doping methods. *ACS Sustainable Chem. Eng.* **2019**, *7* (17), 14647−14660.
(221) Younas, M.; Loong Kong, L.; Bashir, M. J.; Nadeem, H.; Shehzad, A.; Sethupathi, S. Recent advancements, fundamental challenges, and opportunities in catalytic methanation of CO_2. *Energy Fuels* **2016**, *30* (11), 8815−8831.
(222) Mutz, B.; Belimov, M.; Wang, W.; Sprenger, P.; Serrer, M.-A.; Wang, D.; Pfeifer, P.; Kleist, W.; Grunwaldt, J.-D. Potential of an alumina-supported Ni_3Fe catalyst in the methanation of CO_2: Impact of alloy formation on activity and stability. *ACS Catal.* **2017**, *7* (10), 6802−6814.
(223) Shen, L.; Xu, J.; Zhu, M.; Han, Y.-F. Essential role of the support for nickel-based CO_2 methanation catalysts. *ACS Catal.* **2020**, *10* (24), 14581−14591.
(224) Vrijburg, W. L.; Moioli, E.; Chen, W.; Zhang, M.; Terlingen, B. J.; Zijlstra, B.; Filot, I. A.; Züttel, A.; Pidko, E. A.; Hensen, E. J. Efficient base-metal NiMn/TiO_2 catalyst for CO_2 methanation. *ACS Catal.* **2019**, *9* (9), 7823−7839.
(225) Zheng, Q.; Farrauto, R.; Chau Nguyen, A. Adsorption and methanation of flue gas CO_2 with dual functional catalytic materials: a parametric study. *Ind. Eng. Chem. Res.* **2016**, *55* (24), 6768−6776.
(226) Arellano-Trevino, M. A.; Kanani, N.; Jeong-Potter, C. W.; Farrauto, R. J. Bimetallic catalysts for CO_2 capture and hydrogenation at simulated flue gas conditions. *Chem. Eng. J.* **2019**, *375*, 121953.
(227) Duyar, M. S.; Treviño, M. A. A.; Farrauto, R. J. Dual function materials for CO_2 capture and conversion using renewable H_2. *Applied Catalysis B: Environmental* **2015**, *168*, 370−376.
(228) Bermejo-López, A.; Pereda-Ayo, B.; González-Marcos, J.; González-Velasco, J. Ni loading effects on dual function materials for capture and in-situ conversion of CO_2 to CH_4 using CaO or Na_2CO_3. *Journal of CO2 Utilization* **2019**, *34*, 576−587.
(229) Jo, S. B.; Woo, J. H.; Lee, J. H.; Kim, T. Y.; Kang, H. I.; Lee, S. C.; Kim, J. C. A novel integrated CO_2 capture and direct methanation

process using Ni/CaO catal-sorbents. *Sustainable Energy & Fuels* **2020**, *4* (9), 4679−4687.
(230) Jo, S.; Lee, J. H.; Kim, T. Y.; Woo, J. H.; Ryu, H.-J.; Hwang, B.; Lee, S. C.; Kim, J. C.; Gilliard-AbdulAziz, K. L. A fundamental study of CO_2 capture and CH_4 production in a rapid cyclic system using nickel-lithium-silicate as a catal-sorbent. *Fuel* **2022**, *311*, 122602.
(231) Park, S. J.; Bukhovko, M. P.; Jones, C. W. Integrated capture and conversion of CO_2 into methane using $NaNO_3$/MgO+ Ru/Al_2O_3 as a catalytic sorbent. *Chem. Eng. J.* **2021**, *420*, 130369.
(232) González-Castaño, M.; Dorneanu, B.; Arellano-García, H. The reverse water gas shift reaction: a process systems engineering perspective. *Reaction Chemistry & Engineering* **2021**, *6* (6), 954−976.
(233) Bobadilla, L. F.; Riesco-García, J. M.; Penelás-Pérez, G.; Urakawa, A. Enabling continuous capture and catalytic conversion of flue gas CO_2 to syngas in one process. *Journal of CO2 Utilization* **2016**, *14*, 106−111.
(234) Sun, H.; Wang, J.; Zhao, J.; Shen, B.; Shi, J.; Huang, J.; Wu, C. Dual functional catalytic materials of Ni over Ce-modified CaO sorbents for integrated CO_2 capture and conversion. *Applied Catalysis B: Environmental* **2019**, *244*, 63−75.
(235) Jo, S. B.; Woo, J. H.; Lee, J. H.; Kim, T. Y.; Kang, H. I.; Lee, S. C.; Kim, J. C. CO_2 green technologies in CO_2 capture and direct utilization processes: methanation, reverse water-gas shift, and dry reforming of methane. *Sustainable Energy & Fuels* **2020**, *4* (11), 5543−5549.
(236) Hu, J.; Hongmanorom, P.; Galvita, V. V.; Li, Z.; Kawi, S. Bifunctional Ni-Ca based material for integrated CO_2 capture and conversion via calcium-looping dry reforming. *Applied Catalysis B: Environmental* **2021**, *284*, 119734.
(237) Tian, S.; Yan, F.; Zhang, Z.; Jiang, J. Calcium-looping reforming of methane realizes in situ CO_2 utilization with improved energy efficiency. *Science Adv.* **2019**, *5* (4), No. eaav5077.
(238) Kim, S. M.; Abdala, P. M.; Broda, M.; Hosseini, D.; Copéret, C.; Müller, C. Integrated CO_2 capture and conversion as an efficient process for fuels from greenhouse gases. *ACS Catal.* **2018**, *8* (4), 2815−2823.
(239) Jo, S.; Lee, J. H.; Woo, J. H.; Kim, T.-Y.; Ryu, H.-J.; Hwang, B.; Kim, J. C.; Lee, S. C.; Gilliard-AbdulAziz, K. L. Coke-promoted Ni/CaO catal-sorbents in the production of cyclic CO and syngas. *Sustainable Energy & Fuels* **2021**, *6* (1), 81−88.
(240) Ball, M.; Weeda, M. The hydrogen economy - Vision or reality? *Int. J. Hydrogen Energ* **2015**, *40* (25), 7903−7919.
(241) Khan, M. H. A.; Daiyan, R.; Neal, P.; Haque, N.; MacGill, I.; Amal, R. A framework for assessing economics of blue hydrogen production from steam methane reforming using carbon capture storage & utilisation. *Int. J. Hydrogen Energ* **2021**, *46* (44), 22685−22706.

■ NOTE ADDED AFTER ASAP PUBLICATION

This paper was originally published ASAP on June 9, 2022, with an incorrect Figure 13A. The revised version was reposted on June 10, 2022.

https://doi.org/10.1021/acscatal.2c01646
ACS Catal. 2022, 12, 7486−7510